Seasonal dynamics of organic carbon and metals in thermokarst lakes from discontinuous permafrost zone of western Siberia

R.M. Manasypov[1], S.N.Vorobyev[1], S.V. Loiko[1], I.V. Kritzkov[1], L.S. Shirokova[2,3], V.P. Shevchenko[4], S.N. Kirpotin[1], S.P. Kulizhsky[1], L.G. Kolesnichenko[1], V.A. Zemtzov[1], V.V. Sinkinov[1], O.S. Pokrovsky[1,2]*

[1] Tomsk State University, 634050, Tomsk, 36 Lenin av., Russia

[2] Geosciences and Environnement Toulouse, UMR 5563 CNRS, Université de Toulouse, 14 avenue Edouard Belin, 31400, France, oleg@get.obs-mip.fr

[3] Institute of Ecological Problems of the North UroRAS, 163061, Arkhangelsk, Nab. Severnoj Dviny, 23, Russia

[4] P.P. Shirshov Institute of Oceanology of the Russian Academy of Sciences, 36 Nakhimovsky Prospekt, 117997 Moscow , Russia

Key words: boreal, subarctic, palsa, ice, freezing, winter, spring, trace element

Abstract

Despite relatively good knowledge of the biogeochemistry of Siberian thermokarst lakes during summer base flow, their seasonal dynamics remains almost unexplored. This work describes chemical composition of ~130 thermokarst lakes ranging in size from few m² to several km², located in the discontinuous permafrost zone. Lakes were sampled during spring flood, just after the ice break (early June), the end of summer (August), the beginning of ice formation (October) and during full freezing season in winter (February). The lakes larger than 1000 m² did not exhibit any statistically significant control of the lake size on Dissolved Organic Carbon (DOC), the major and trace element concentrations over three major open water seasons. On the annual scale, the majority of dissolved elements including organic carbon increased their concentration from 30 to 500% with statistically significant ($p < 0.05$)

trend from spring to winter. The concentration of most trace elements (TE) increased in the order spring > summer > autumn > winter. The ice formation in October included several stages: first, surface layer freezing followed by crack (fissure) formation with unfrozen water from the deeper layers spreading over the ice surface. This water was subsequently frozen and formed layered ice rich in organic matter. As a result, the DOC and metal (Mn, Fe, Ni, Cu, Zn, As, Ba and Pb) concentrations were the highest near the surface of the ice column (0 to 20 cm) and decreased by a factor of 2 towards the bottom. The main implications of discovered freeze-driven solute concentrations in thermokarst lake waters are enhanced colloidal coagulation and removal of dissolved organic matter and associated insoluble metals from the water column to the sediments. The measured distribution coefficient of TE between amorphous organo-ferric coagulates and lake water (< 0.45 µm) were similar to those reported earlier for Fe-rich colloids and low molecular weight (< 1 kDa, or < 1-2 nm) fraction of thermokarst lake waters, suggesting massive co-precipitation of TE with amorphous Fe oxyhydroxide stabilized by organic matter. Although the concentration of most elements was lowest in spring, this period of maximal water coverage of land created significant reservoir of DOC and soluble metals in the water column that can be easily mobilized to the hydrological network. The highest DOC concentration observed in smallest (< 100 m²) water bodies in spring suggests their strongly heterotrophic status and therefore, potentially elevated CO_2 flux from the lake surface to the atmosphere.

1. Introduction

Western and central Siberia’s thermokarst (thaw) lakes extend over a territory spanning over a million km² (half of the western Siberia Lowland, 0.5 million km² and all northern Siberia Lowland, 0.84 million km²). They are highly dynamic hydrochemical systems that receive chemical elements from the atmosphere and surrounding peat soil and exchange greenhouse gases (GHG) with the atmosphere, delivering dissolved carbon and metals to adjacent hydrological systems. Because more permafrost will continue to thaw due to climate warming, which is heavily intensified in this region (Frey and Smith, 2005), the directions and magnitude of lakes – rivers exchange processes may be significantly modified, seriously affecting the biogeochemical fluxes both on land and in the coastal zone of the Arctic Ocean.

In contrast to the relatively good understanding of western Siberia thermokarst lakes functioning during active (summer) season (Walter et al., 2006, 2008; Walter Anthony et al., 2012; Audry et al., 2011; Pokrovsky et al., 2011, 2013, 2014; Shirokova et al., 2009, 2013; Karlsson et al., 2012, 2014; Manasypov et al., 2014), the intra-annual variations of lake water chemistry including glacial period and spring flood remained, up to present time, virtually unexplored. At the same time, glacial season is extremely important in GHG regulation in boreal and subarctic lakes, due to significant accumulation of gases under the ice and their liberation during the ice melting (Karlsson et al., 2013). Similarly, the ice formation period provides important insights into the solute concentration and colloid coagulation mechanisms, given the main particularity of shallow (0.3 to 1.0 m deep) thermokarst lakes in western Siberia – their full freezing during winter (Pokrovsky et al., 2011, 2014). The possibility of complete freezing of western Siberia thermokarst lakes contrasts the majority of other circumpolar water bodies, such as from the Kolyma low land (Walter Anthony et al., 2014), the Lena Delta (Boike et al., 2013) and Mackenzie Delta plain (Tank et al., 2009, 2011; Grosse et al., 2013; Walter Anthony and Anthony, 2013) which often have a depth of more than 2 meters and as such do not freeze to the bottom, while exhibiting chemical and thermal stratification of the water column. Another important difference of thermokarst western Siberia lakes from well studied river delta / river valley lakes is the lack of connection to the underground network in the formers. Therefore, lake connection to the hydrological network may occur only via surface flow (Kirpotin et al., 2008), without subsurface flow. Among all studied circumpolar water bodies, shallow ponds of the north of

Canada (Laurion et al., 2010; Negandhi et al., 2013; Bouchard et al., 2014) seem to be most similar to western Siberian thermokarst lakes. However, in a recent compilation of studied circumpolar ponds (Rautio et al., 2011), only one region among 16 (thaw ponds of Boniface, Quebec) exhibits a pH of 5.4±0.6, Cond. of 18 µS cm^{-1} and a DOC of 13.4±4.7 which is comparable to highly diluted ($5 < Cond < 20$ µS cm^{-1}), acidic $3.5 \leq pH \leq 5.5$, and humic and ($10 \leq DOC \leq 40$ mg/L) western Siberia water bodies.

Towards filling the gap in our knowledge of seasonal variations of thermokarst lake chemical composition, we present in this work results of analysis of water and ice sampled in thermokarst lakes of various size, from several meteres to several km in diameter, during four main hydrological seasons: June, August, October and February. Our primary goal was to better understand the thermokarst lake biogeochemical functioning which should allow to constrain the impact of lake water metal and carbon cycling on river water composition and greenhouse gas exchange with the atmosphere in the course of year. On a larger perspective, we aimed at the understanding seasonal pattern of dissolved organic carbon and metal micronutrient concentration in these shallow but highly abundant water bodies, different from previously studied glacial and deep thermokarst/yedoma lakes. This knowledge should allow predictions of phytoplankton activity, sedimentation and microbial respiration on the annual scale, necessary for evaluation of the net ecosystem exchange under various climate change scenarios. To this end, we adressed the following specific questions: (i) is there a statistically significant difference in major and trace element concentration between different seasons, within a broad range of lake sizes? (ii) how significant is lake size and lake water residence time control for lake water chemical composition during different seasons? (iii) what are the mechanisms and degrees of element differentiation during ice formation and full water column freezing? (iv) how significant is water dilution during spring melt and what are the consequences for river water feeding by lakes during this period?

2. Study site description, sampling, analytical and statistical methods.

Our study site is located in the central part of Western Siberia (63.5°N, 75.4°E, Nojabrsk administrative region) withing the northern taiga geographical sub-zone (**Fig. 1**). It contains discontinous permafrost over Late Pleistocene sand and clay deposits that are covered by a layer of peat that is 1–2 m thick. All the lakes in this study are located at watershed divides between adjacent rivers. The water bodies ranged from a few m to several km in diameter and had a similar depth of 1.0 ± 0.5 m under normal precipitation/evaporation conditions (450 mm). During dry summer, the lakes can decrease their depth twofold (Pokrovsky et al., 2013). The morphology, hydrology and the water balance of thermokarst lakes have been extensively studied during four field campaigns in June, August, and October 2013 and February 2014. The detailed depth mapping of ~20 large lakes was performed via GPS-echosounder from a rubber boat; the denivelation and the direction of the water flow were measured using levelling network in several narrow profiles; the depth and density of snow were measured over a model site 500 m x 500 m that included lakes, palsa bog, some streams and adjacent forested riparian zone. The water residence time was calculated from the annual precipitation and evapotranspiration measured at the neighboring meteostation of the Russian Hydrometeorological Station, the annual runoff of the territory (between 200 and 250 mm, Novikov, 2009 and Frey et al., 2007) and the water volume of the lakes measured on-site using a GPS-echosounder.

Water samples were collected from the PVC boat for large lakes or directly from the lake center for small (< 50 m diameter) water bodies (thaw ponds) during June and August 2013 and from the ice during October 2013 and February 2014 sampling campaigns. A list of sampled water bodies and their main hydrological and hydrochemical characteristics is presented in Table 1. The sampling and filtration methods used in this study, as well as the chemical analysis techniques, are identical to those utilized in our previous studies (Pokrovsky et al., 2011). An ultraclean sampling procedure was used for all manipulations in the field (Shirokova et al., 2010). Water samples were filtered on-site through sterile single-use Minisart® filter units (Sartorius, acetate cellulose filters) with a pore size of 0.45 µm. For TE analysis, samples were acidified to pH = 2 with double distilled HNO_3. Dissolved oxygen, pH, and Eh were measured on-site with uncertainties of 5%, 0.02 units, and 2 mV, respectively, using a WTW® oximeter and a Hanna® portable pH meter with an Eh/pH electrode.

Major anion concentrations (Cl^- and SO_4^{2-}) were measured by ion chromatography (HPLC, Dionex ICS 2000) with an uncertainty of 2%. DOC was analyzed using a Carbon Total Analyzer (Shimadzu TOC 6000) with an uncertainty lower than 3%. Major and trace elements were determined with an ICP-MS Agilent ce 7500, routinely used in our laboratory for the analysis of samples from boreal organic-rich lakes (cf. Pokrovsky et al., 2013). Indium and rhenium were used as external standards. The international geostandard SLRS-5 (Riverine Water Reference Material for Trace Metals certified by the National Research Council of Canada) was used to check the accuracy and reproducibility of each analysis (Yeghicheyan et al., 2014). We obtained good agreement between replicate measurements of SLRS and certified values (relative difference < 10% SD for repeated measurements), except for B and P (30%). While P was discarded for further analyses, B concentrations in most lakes are a factor of 3 to 7 higher than those in the SLSRS-5 and thus were retained. In addition to TE analysis using the Agilent quadropole instrument, 60% of samples were processed with an ultrasensitive Element XR ICP-MS instrument operated in a low and medium resolution mode. Using this ICP-MS greatly increased the detection limits of a number of elements and improved the precision of the analyses while avoiding interferences. The uncertainty of the Element XR analysis was ≤ 5%, while its detection limit was a factor of 100 lower than the traditional (Agilent) instrument. The average agreement between the two ICP-MS instruments for the majority of the TE was 10-15%.

The lake ice was sampled in February 2014 from the central part of the lakes using titanium circular ice coring. The ice core was cut using Ti saw in 10-cm slices, melted at room temperature and immediately filtered through 0.45-µm filters. Before and after fieldwork, blank samples were run by filling the pre-cleaned PVC container with MilliQ water and submerged Ti blades, at neutral pH and letting it to react for several hours. No detectable contamination of Ti, any major and trace elements was observed. The ice filtrate was processed in the same way as the lake water. In three lakes (out of ~ten studied in February), the bottom layer of unfrozen water below the ice column was collected for analysis. Chemical composition of Fe-rich coagulates collected from the ice surface in early June was measured by ICP-MS after full dissolution of the solid using a microwave acid digestion procedure (Stepanova et al., 2014). Particulate organic carbon was quantified using $\mathrm{TOC_{CHS}}$ instrument. The freeze-dried precipitates were characterized by scanning electron microscopy (SEM) using a Jeol JSM840a, and by X-ray diffraction using an INEL CPS 120 CoKα.

The element concentrations were analysed using best fit functions based on the least squares method, Pearson correlation and one-way ANOVA (SigmaPlot version 11.0/Systat Software, Inc). Regressions and power functions were used to examine the relationships between the elemental concentrations and the lake surface areas. The ANOVA was carried out using Dunn's method because each sampling period contained different number of water bodies. Principal component ananlysis (PCA) was used for the ensemble of sampled lakes and for each season individually, to reduce the number of variables and to detect the structure in the relationships between the elements. The data consisted of ~130 lake water samples grouped into three distinct seasons (spring, summer and autumn). Statistical PCA analyses were applied in order to derive a distinctive view of the influence of various parameters, notably the seasons, on the lake water chemical composition variability. Both normed and non-normed PCA treatment was attempted. Statistical analysis considered each chemical element as a variable (35 in total) for all lakes. For this step, the STATISTICA package (http://www.statsoft.com) which is also designed to compute and render graphics, was used to interpret the spatial structures.

3. Results

3.1. Effect of the lake size on dissolved carbon and related elements concentration in the water column.

The list of sampled water bodies with their main hydrophysical and hydrochemical characteristics and their geographical localization are given in **Table 1 and Fig. 1**, respectively. Within the range of 100 to 2×10^6 m² lake size, the effect of lake size on major and trace element concentration is not strongly pronounced. The correlation coefficient was below 0.5 for all elements over all seasons, suggesting a quite weak if not negligible impact of the lake size on lake water chemical composition (**Table S1 of the suppelment)**.

Highly variable number of sampled lakes during each season was basically due to the difficulties in sampling logistics and the access to the site. Only five lakes (labelled A, B, C, D, E in Table 1) could be collected during all three open water seasons. In winter, we could not sample more than 3 lakes (both ice core and bottom water). All small lakes (< 1000 m²) were frozen solid in October (autumn period). We did not focus in this work on small size (< 500 m²) lakes in summer, because the small water objects were thoroughly studied in our previous work (Shirokova et al., 2013). Besides, many small ponds (10-100 m²) were dried in August 2013. For this reason, the size range of the sampled lakes is different among seasons.

Only in spring, for the range of 0.1 to 2×10^6 m² lake size, was Pearson's coefficient statistically significant ($p < 0.05$) and suggested a decrease of the following element concentration with the logarithm of the lake size increase: DOC (-0.69), V (-0.43), Cr (-0.54), Ni (-0.58), Cu (-0.63), Ga (-0.71), As (-0.53), Cd (-0.69), Pb (-0.8)**.** Such a semi-logarithmic negative relationship suggests a rapid decrease in the concentration within the small water bodies and its relative stability in large lakes. Indeed, this trend was mainly due to the increase of certain element concentrations in the smallest (< 10-100 m²) water bodies rather than a steady evolution of concentrations in medium-size and large water bodies.

The DOC concentration exhibited two maxima, at 1000-10,000 m² surface area in summer and autumn and in micro-depressions (< 1 m²) in spring (**Fig. 2**). The nature of the DOC was different among different seasons, because the slope of the UV_{280} - [DOC] dependence increased in the order: spring (0.024) < summer (0.030) < autumn (0.035) < winter (0.0354). The ratio of UV_{280} to [DOC] during 4 sampled seasons demonstrated the lowest values in spring and the highest in Fall-winter, being independent of the lake size (**Fig. 3**).

None of the season demonstrated a statistically significant dependence between the element concentration and the water body size above 100 m² ($p > 0.05$). There was quite high variability in the major element concentration in lakes of the same size range, typically over 2 orders of magnitude, as can be seen for Ca and Si in **Fig. S2 a and b (Supplement),** respectively. There was a general increase in the lake water pH with the increase in the lake size (statistically significant at $p < 0.05$), most visible during summer (**Fig. 4**). The small-size lakes sampled in spring exhibited the lowest pH, between 3.5 and 4.5 whereas the larger lakes (> 1000 m²) in summer demonstrated a pH of 5 to 6. Similar to major cations, the major anion concentration did not demonstrate any discernable trend ($p > 0.05$) with the lake surface area; only Cl^- yielded the minimal concentration for the lakes of c.a. 100 m² surface area. Dissolved inorganic carbon (DIC) concentration was a factor of 30 lower than [DOC], without statistically significant trend with the lake size (not shown). The illustration of the lake surface area effect on trace element concentration during all four sampled seasons is given in **Fig. S3** in the Supplement for Fe, Al, Mn, Zn, Cu, Pb, Mo, V, As, and Sb and the primary data are listed in **Table S2**.

There was limited degree of element correlation with either DOC or Fe considering all seasons of the year, as follows from Pearson pair correlation (**Table S3**). Examples of mostly pronounced correlations between Fe and DOC, As and Fe, and Cd and DOC are illustrated in **Fig. S4.**

The statistical treatment of the data did not reveal significant ($p > 0.05$) links between TE concentration and UV280 nm. Rather poor correlations shown in Fig S4 (Supplement) of the manuscript are illustrative for both UV and DOC. The concentration of TE in peat unfrozen horizon and in ground vegetation (green and brown mosses) in the discontinuous permafrost zone of western Siberia are rather similar (Stepanova et al., 2015). As a result, UV_{280} can help to distinguish between the element leaching from vegetation as opposed to peat leaching. Rather, the similarity of specific UV absorbances across the seasons and lake size strongly suggests the dominance of terrestrial (soil and litter) sources of OC with minimal aquagenic DOM.

Considering all seasons simultaneously, several groups of elements could be distinguished based on this correlation analysis:

(i) elements correlated with Fe ($R_{Fe} > R_{DOC}$): Cl, SO_4, Mg, Ca, Sr, Ba, Rb, Al, Ga, Cr, Mn, Co, Ni, Si, As, REEs and U

(ii) elements correlated with DOC rather than with Fe ($R_{DOC} > R_{Fe}$): Cu, Zn, Cd and Pb

(iii) elements strongly correlated to Al ($R > 0.6$ at $p < 0.05$): Be, Si, K, Rb, Cs, Sr, Ba, Ti, V, Cr, Co, Cu, Ga, As, Sb, REEs, W and U

(iv) elements exhibiting high pair correlations ($R \geq 0.9$ at $p < 0.05$): Ga-Al, Cr-Al, Hf-Th

Note that all elements exhibited better inter-correlations in spring compared to other seasons (**Table S3**).

3.2. Lake freezing during the glacial period (October to the end of May) and ice-layered structure formation

Observations during the beginning of the ice formation (October 2013) yielded important and novel features of thermokarst lake ice cover evolution during glacial period. Given the closed basins of all sampled lakes underlain by permafrost without connection to the groundwater source (i.e.., Pokrovsky et al., 2011, 2014), the water was expected to be under excess pressure under the ice. This was confirmed by direct observations in October: the water always rose upward and spread over the ice surface after drilling the first 10-20 cm of the ice layer. Upon the thickening of the ice, cracks formed on the ice cover and the water from the deeper layers seeped and spread over the ice surface, thus forming organic- and Fe-rich multilayered ice up to 30 cm thick. The wind acting on still unfrozen freshly ejected water created ice ripples spreading over a surface of 10-50 m^2 (**Fig. S5**). The full freezing of ejected organic-rich water led to browning of the ice and presumably produced significant coagulation of colloids. The products of this coagulation could be notably seen at the end of the spring, during massive ice melt (**Fig. S6**).

In-situ oxygen analysis with submersible O_2 sensor in June and August demonstrate saturation with atmospheric oxygen close to 90 ± 10% (**Table 1**). In October, under the ice, we found only 40-80% saturation of the water layer, with some redox stratification within 20-50 cm of the unfrozen water column. There was a 50% drop in O_2 concentration at the sediment-water interface relative to the bottom of the ice core. Generally, the smaller the water body, the lower the oxygen concentration, although a straightforward relation between the size of the lake and the oxygen saturation in October could not be established ($p > 0.05$).

The ice core analysis with the resolution of 5-10 cm demonstrated either an enrichment of the surface ice layers in dissolved elements, or their non-systematic variation over the full depth of the ice core (**Table S4**). The enrichment, by a factor of 2 to 5, of the first 0-30±10 cm was detected for DOC and most metals such as Al, Fe, Ni, Co, Cu, Zn, Pb as illustrated for selected metals in **Fig. 5**. Manganese demonstrated the largest variation along the ice core depth. Its concentration decreased from 3 to 10 ppb at the very surface down to less than 0.1 ppb below 50 cm. In contrast, many trace elements (Cd, Cs, Sb, Ti, Zr, Hf, Th, U, REEs) did not demonstrate statistically significant ($p < 0.05$) trend of concentration with depth for three sampled ice cores. Ca^{2+}, SO_4^{2-}, DIC, Cl^-, and Na^+ also demonstrated nonsystematic variation with depth. In winter, only three (out of ~ ten) sampled lakes yielded the liquid water presence above the sediment. The thickness of the unfrozen layer ranged from 10 to 20 cm, with an ice thickness of 60 to 80 cm.

Using the element concentration measured in remaining water at the sediment – ice interface and the bottom 10 cm layer of the ice core, element distribution coefficients between the ice and the remaining fluid can be assessed. Note that the obtained values can be considered as preliminary estimations, given very limited number of samples. The agreement in K_d (water/ice) between three sampled lakes for which both fluid and bottom ice were available is reasonably good for a number of major elements, as it can be seen from the average with 2 SD ($n = 3$) listed in **Table 2.** The lowest K_d (water/ice) is observed for DIC (1.64±0.37) and Cl (7.6±3.0). The DOC distribution varied significantly among the lakes (K_d (water/ice) is between 5 and 21). Al, Ti, Mn, Ce and some REE yielded K_d (water/ice) between 50 and 100. The majority of other trace elements exhibit the K_d (water/ice) between 10 and 40 without any discernable link to element chemical properties and degree of binding to DOM.

The most significant transformation of the lake water chemical composition presumably occur during the full freezing of the water column over the winter period. At the end of the winter, during massive snowmelt, products of colloidal coagulation are largely present at the surface of the ice blocks within the lake borders (**Fig. S6**). The coagulates collected in large (~10^6 m^2) thermokarst lakes in early June are essentially composed of iron oxohydroxide and organic matter with significant amount of co-precipitated trace elements. The aggregates are XRD-amorphous and contain 17.5±0.5% of POC.

Based on total chemical analysis of solid coprecipitates, we calculated the distribution coefficients of trace element (TE) between the Fe-rich coagulates and the lake water, normalized to Fe (as the major component of the coagulates):

$$K_d = [TE]/[Fe]_{coagulate} / [TE]/[Fe]_{lake\ water}$$

where $[TE]/[Fe]_{lake\ water}$ represents the ratio of average TE and Fe concentrations in large lakes at the end of summer, before the beginning of ice formation. The K_d values of major and trace elements range from 0.05 to 0.5 (**Fig. 6**). Although based on limited number of samples, the values of distribution coefficient obtained in the present study are in reasonable agreement with those reported for colloids (1 kDa – 0.45 µm) and LMW (< 1 kDa) fraction of another large thermokarst lake located in discontinuous permafrost zone (Pokrovsky et al., 2011) as well as the rivers and streams of the boreal non-permafrost zone (Vasyukova et al., 2010). For the majority of dissolved elements, the K_d of particles are within a factor of 2 different from previously reported K_d of colloids.

3.3. Seasonal trend in element concentration in the thermokarst lake water: progressive increase from June to February

The first statistical test was aimed to assess the difference in element concentration between different seasons for the full range of the lake size. It was found, using H-criterion of Kruskal–Wallis and Mann-Whitney U Test, which allowed one to estimate the difference between two independent set of data based on one given parameter, that all elements are different between three main seasons at the significance level of $p < 0.05$. This allowed one to calculate the average element concentration with $\pm 2\sigma$ standard deviation or all studied lake sizes from 100 to > 500,000 m² for spring, summer and autumn, as listed in **Table 3**. Note that the winter data are of low representativity, given that only three unfrozen lakes could be used for this calculation. The median was similar to the average within the 2σ standard deviation of the average.

The majority of dissolved elements exhibited a statistically significant increase of their average concentration from spring to autumn (20 to 50%). These are DOC, Mg, K, Ca, Al, Ti, V, Cr, Mn, Fe, Ni, Co, Cu, Ga, Rb, Sr, As, Cd, Sb, Mo, Cs, Ba, all REEs, Pb, and U. Examples of the average element concentration evolution grouped by several families of elements with similar chemical properties and affinity to DOC and Fe colloids (i.e., Pokrovsky et al., 2013) are shown in **Fig. 7.** The trends of element concentration in the lake water from spring to autumn are quite similar for large (> 500,000 m²) and medium (100-500,000 m²) water bodies. We estimated the minimal impact of lake water freezing assuming a conservative scenario of element concentration evolution in thermokarst lakes. Based on thorough hydrological observations, we accepted, for 1 m^2 of the average lake depth of 75±25 cm in summer, to which we added 20 cm flooding in spring and from which we subtracted 20 cm of the water layer for ice formation in October. The 3 sampled lakes exhibited almost full freezing in February with c.a. 10 cm of bottom water left and 65 cm of the ice. The concentration factor was calculated as the ratio of the water volume under 1 m^2 in a given season to that in spring. It was equalled to 1, 1.3, 2.0 and 9.5 for June, August, October and February, respectively.

Conservative behavior of selected major and trace elements is illustrated in **Fig. 7** as a dashed line. Most major elements (Si, K) and a number of trace metals (Al, Ti, Cr, Cu) exhibited close to conservative behavior. In contrast, DOC demonstrated significant depletion during winter, between October and February. Fe, Ni, Cd and Pb were slightly non-conservative showing a depletion in winter. The effect of the season can be quantified as the ratio of the average summer and autumn to spring concentration ($R_{\text{summer/spring}}$). This ratio is the highest for Ba (6.7) and light REEs (7 to 3), followed by Zn (4.3), Si (4.3), Al, Fe and trivalent hydrolysates (4.2 to 2.8), tetravalent hydralysates, Cr and divalent heavy metals such as Co, Cu, Ni, Cd, Mn (2.5 to 3.3). A number of elements did not demonstrate a significant increase in the concentration during the baseflow season compared to the spring period, exhibiting $R_{\text{summer/spring}}$ values below 2 (B, Mg, Na, Ca, Cs, Pb, V, As, Sb, Th and Zr). This empirical result helps to distinguishe two groups of elements: elements whose concentrations are affected by the seasons by a factor of 2 or higher and elements do not significantly increasing their concentration in summer relative to the spring seasons. For example, the increase of Si and metal micronutrients (Zn, Co, Ni, Cu, Cd, Ba and Mn) might indicate some preferential release of these elements during active plant and upper moss litter leaching in summer. High concentrations of B, Na, Mg, Ca, Cs, Pb in early spring relative to the end of summer may indicate their input with atmospheric precipitates.

Despite significant uncertainty in the average summer-period element concentration in thermokarst lakes (see **Table 3**), the values obtained in the present study are consistent with thermokarst lake water chemical composition across the gradient of the permafrost zone, from discontinuous/sporadic to continuous permafrost. The values of DOC, all major and trace element concentration agree, within the uncertainty of the average, with the values of element concentration interpolated from the latitude – lake water concentration dependence (Manasypov et al., 2014) for the latitude of the study site. It follows that relatively small area investigated in this work can be a good surrogate for much larger region of western Siberia (described in Manasypov et al., 2014) in terms of seasonal evolution of thermokarst lake chemical composition.

3.4. Water residence time effect on lake water chemical composition

The effect of lake water residence time (WRT) on the summer-period and average spring-autumn chemical composition of thermokarst lakes exhibits two clusters of the data points (**Fig. 8**). Statistical analysis of observed dependencies confirmed a significant link between the water residence time and both summer and season-average DOC concentrations with the Spearman correlation coefficient (R_S) equal to -0.65 ($p < 0.05$). The most important result is that, at WRT < 8 months, an almost five-fold increase in DOC concentration occurs. A similar impact is observed for Fe with $R_S = -0.55$ ($p < 0.05$). This result can be understood given that the Fe is likely to be present in the form of organic colloids. The alkaline and alkaline-earth major cations and other metals, however, did not demonstrate any statistically significant ($p > 0.05$) link to the WRT. The estimation of WRT for the smallest (< 10-100 m^2) water bodies was impossible due to the ephemeral nature of these small thaw ponds. However, considering their typical existence between the start of the snow melt (May) and summer drought (July – August), the water resides in these water bodies between 0.1 and 0.3 years. The highest concentration of DOC observed in spring in < 10 m^2 depressions **(Fig. 2)** is therefore consistent with the trend shown for large lakes in **Fig. 8.**

3.5. PCA analysis of possible TE sources in thermokarsk lakes

The data consisted of ~130 lake water samples grouped into three distinct seasons (spring, summer and autumn). Statistical analysis considered each chemical element as a variable (35 in total) for all lakes. Considering all seasons together, the first factor was responsible for 16% variation and included B, Na, Si, K, Ca, Ti, V, Cr, Ni, Zn, Rb, Mo, Sb, Cs, Ba, La, Ce and U whereas the 2nd factor (6.3%) included Al, Fe, Co, As, and Cd (**Fig. S7**). Separation of F1 and F2 factors in June and August was uncertain since they provided only 9% and 6.7% (June) and 11.8% and 5.8% (August) variations. In contrast, October's data could be explained by 18.8% variation of F1 (B, Na, Si, K, Ca, Ti, V, Cr, Ni, Zn, Rb, Sr, Zr, Mo, Sb, Cs, Ba, La, Ce and U) and 4.4% F2 (SO4, Cu, Co, Fe, As). The list of elements and corresponding factors for each season are given in **Table S5.**

This PCA treatment demonstrated rather high variability of lake chemical composition, mostly pronounced during June and August. In June, multiple factors are responsible for element enrichment in the lake water, namely the lateral input from thaw snow and lake ice, dissolution of colloid coagulation products, and leaching of plant litter. The F1 factor in June is very poorly pronounced. Nevertheless, it may mark the colloidal transport of TE (organic complexes) whereas the 2nd factor may correspond to the degree of snow input (typical atmospheric aerosol – originated elements). In August, internal (autochthonous) processes and subsurface feeding are likely to strongly modify lake water chemical composition both for major (pH and DIC of the F2 factor) and TE. In addition, atmospheric precipitation in the form of rain which dilute lithogenic TE but also deliver marine aerosols and dust (subjected to dissolution) can strongly modify the role of individual correlations. Finally, October represents the period when the first factor is mostly pronounced, as also translated in the PCA results of all seasons together. Presumably, the period of the beginning of ice formation corresponds to the maximal stability of the F1 x F2 structure; during this time, the influence of both allochthonous (lateral and subsurface TE influx from peat, mineral soil horizons and ground vegetation) and autochthonous (bio- and photodestruction of organic colloids, primary productivity) processes are minimal.

3.6. Element speciation in thermokarst lake waters

We used the geochemical program Visual MINTEQ (Gustafsson, 1999), version 3.1 (October 2014)) for Windows, (see Unsworth et al. (2006) for vMINTEQ application example) in conjunction with a database and the NICA-Donnan humic ion binding model (Benedetti et al., 1995; Milne et al., 2003) and Stockholm Humic Model (SHM). Speciation calculations were performed for Ba, Ca, Cd, Co, Cu, K, Mg, Mn, Na, Ni, Pb, Sr, Zn, and Al, Fe^{III}, Th^{IV}, and $U^{VI}O_2$ for average lake water composition in spring, summer, autumn and winter as well as the average August composition of large (> 500,000 m^2) and small (100-500,000 m^2) lakes (Table 3). In addition to NICA-Donna approach, Stockholm Humic Model (SHM) of visual MINTEQ was used to calculate metal speciation in the lake water.

Results of the calculation of metals degree of complexation with DOM are listed in **Table S6** and illustrated in **Figures S8 and S9.** According to NICA-Donnan model, the majority of divalent major and trace element is bound to organic, Donnan-like complexes. Only Na and K exhibits a decrease of 80 to 10% complexed fraction from spring to winter. Extremely high complexation of metals with DOM (up to 80 to 90%) within the Nica-Donnan concept is supported by dialysis experiments conducted in various thaw lakes of western Siberian subarctic (Pokrovsky et al., 2013; Shirokova et al., 2013). In contrast to the Nica-Donnan, the Stockholm Humic Model (SHM) predicts moderate and quite variable association of divalent metals with DOM, with the lowest values for Ba and Mn (40% in spring and 20% in winter) and the highest values for Cu and Pb (80-90% for all seasons). It is important to note that the highest proportion of organic complexes is observed in summer, presumably due to the highest pH recorded during this season which favors the deprotonation of functional groups of the DOM. The lowest proportion of organic complexes in winter could be due to competition between metals for organic ligand binding sites, given significant increase of Me^{2+} compared to DOC during solute concentration by freezing.

The lake size has pronounced impact on some metal complexation with DOM as illustrated in **Figure S9.** Even within the “conservative“ SHM model, the TE in small thaw ponds exhibit 100% complexation with DOM. The degree of complexation is smaller in large lakes having a factor of 2 lower DOC concentration, despite that their pH is higher than that of small lakes (5.49 and 4.72, respectively). Interestingly, this may indicate higher bioavailability of metal micronutrients in large lakes, in line with the hydro biological evolution of western Siberia thermokarst lakes, namely the elevated productivity and the presence of macrophytes and phytoplankton blooms in large mature thermokarst lakes (Pokrovsky et al., 2014). Another important conclusion from the speciation modeling is that the DOC concentration has more pronounced impact on metal speciation (notably the % of organic complexes) than the pH - both across the seasons and different lake size groups.

4. DISCUSSION

4.1. Lake water composition control by snow and ice melt in spring.

All trend described in this work on numerous lake analysis are confirmed by the data of 5 lakes sampled throughout the year. This is illustrated for pH, DOC, Al and Cu for the same 5 lakes sampled in spring, summer and autumn. For a large range of lake surface area, the trend spring < summer < autumn is clearly visible and statistically significant ($p < 0.05$).

The lack of a trend in DOC and metal concentration with the lake surface area increase above 1000 m^2 (**Fig. 2, Table S1,** $R^2 = 0.17$, $Rs = -0.33$) in June implies that the lakes are essentially influenced by allochthonous (surface runoff from snowmelt) sources of dissolved material with minimal transformation of DOC and metal complexes by intra-lake autochthonous processes. In the opposite case, one would expect a tendency of DOC and chemical element increase with the decrease of the size of the water body, notably below 100 m², as it is encountered in summer periods in sporadic and discontinuous and permafrost zone of thermokarst lake development (Shirokova et al., 2013). Given that the upper part of the peat column is still frozen in the beginning of June, the source of the solutes to the lake water is most likely to be ground vegetation, comprising dwarf shrubs, mosses and lichens, as well as the litterfall of the previous year. The input of the vegetation leaching products should be similar for the lakes of different sizes, given the very homogeneous palsa bog dominant landscape at the study site.

The spring flood period is known to be the most important in terms of land coverage by water, on the annual scale (Zakharova et al., 2009, 2014). As a result, the average chemical composition of the dominant surface waters in the discontinuous permafrost zone of western Siberia can be approximated by that of the spring period as listed in **Table 3**. Elevated DOC concentration in thermokarst lakes during spring priod, a factor of 2 to 3 higher than the typical 10-15 mg L^{-1} of boreal waters (Dillon and Molot, 1997), suggests high potential of releasing CO_2 to the atmosphere, notably in numerous small depressions filled by thaw water.

A systematic ($p < 0.05$) increase of the average slope of dependence $UV_{280\ nm}$ – [DOC] in the course of the season (**Fig. 3**), from 0.024 in spring to 0.0354 in winter (the latter with only 3 samples) suggests an increase in the input of aromatic compounds (presumably from peat lixiviation) to the end of the vegetative season relative to the leaching of fresh vegetation products (low aromatic, plant and litter exudates) mostly visible after the snowmelt, when the surrounding peat is still frozen. Correcting the UV absorbance for dissolved Fe^{3+} (Weichaars et al., 2003) via subtracting a term of 0.08×[Fe, ppm] will change the $UV_{280\ nm}$ value by less than 10% which is beyond the variability of the seasons and lake size. Note also that a recent study of DOC-UV properties in a boreal site demonstrated the absence of the influence of nitrate and iron on UV and visual absorbance up to 2.2 mg/L of Fe(III), Avagyan et al. (2014). The lack of any trend ($p > 0.05$) in UV/DOC ratio as a function of the lake size (**Fig. 3)** strongly suggests the similarity of the DOC sources in the full range of the lake size in each season. As a result, the season rather than the lake size at $S > 100$ m² seems to be the most important factor controlling both the average concentration and the chemical nature of DOC and related elements.

Comparison of TE concentration in summer relative to spring (section 3.3) distinguishes two groups of elements: elements which do not significantly increase their concentration in summer relative to the spring and elements whose concentrations are affected by the seasons by a factor of 2 or higher. For example, the increase of Si and metal micronutrients (Zn, Co, Ni, Cu, Cd, Ba and Mn) in summer relative to spring might indicate some preferential release of these elements during active plant and upper moss litter leaching in relatively warm waters. In contrast, high concentrations of B, Na, Mg, Ca, Cs, Pb in early spring compared to the end of the summer may indicate their input with atmospheric deposition after snow melt.

4.2. Concentration mechanism during freezing period; enhanced colloidal coagulation

The unusual distribution of organic carbon and related trace elements over the ice core profile, with an accumulation in the upper 20-40 cm of the ice column, stems from a sequence of events during lake freezing, linked to (*i*) shallow depth and possibility of the full freezing of the water column and (*ii*) the lack of any outlet or hydraulic connection to the groundwater of these confined water bodies underlain by the impermeable permafrost layer in the form of the frozen sand/peat. The hypothetical scheme of crystallization process is illustrated in **Figure 9.** The squeezing of remaining water from the bottom towards the surface through the ice cracks starts as early as October. This produces the layered, organic- and Fe-rich secondary (allochthonous) ice which is crystallized at the already frozen lake surface. During winter, the progressive freezing downwards the water column and the decrease in the connectivity between the remaining water and the lake surface bring about the decrease in element concentration in the bottom ice while concentrating of solutes in the remaining fluid at the ice – sediment interface. The progressive lake freezing produces layered ice having contrasted content of major and trace elements among different layers, reflecting the full freezing of water pockets formed via seeping the bottom water at the lake surface. The DOC and many related elements exhibit a general decrease of concentration downward from the ice core surface. The freezing sequence of the thermokarst lakes constrasts with the freezing of non-permafrost (glacial) lakes, which are generally deeper than 1 m and have an inlet/outlet and underground connection. To which degree the scheme of ice formation suggested for shallow thermokarst lakes in discontinuous permafrost zone can be applied to other, sporadic and continuous permafrost regions of western Siberia, remains unknown. However, given shallow depth and closed-basin settings of most thermokarst lakes, the extrapolation of obtained ice chemistry data and partitioning coefficients to other thermokarst lakes of western Siberia should be possible.

To our knowledge, the information on TE partitioning between the lake water and the ice for other boreal settings is lacking. The similar range of DOC and many major and trace metal distribution coefficients between the ice and the remaining solution encountered in the present study (Table 2) is remarquable and contrasts with the recent results of DOM incorporation during sea ice formation (Muller et al., 2013). The latter authors argued that DOM is incorporated to sea ice relatively more than inorganic solutes. In the case of low total dissolved solid (TDS), DOM-rich thermokarst lakes of the present study, the majority of solutes may follow the DOC being present as organic colloids (1 kDa – 0.45 µm), as follows from vMINTEQ speciation calculation (section 3.6) and also demonstrated by dialysis experiments (Pokrovsky et al., 2011, 2013).

Various physico-chemical processes may be involved in the transformation of solutes and DOM and metal-rich water pockets incorporated in the ice, notably within its most surface layers. Among them, photoreductive dissolution of iron oxy(hydr)oxide trapped in the ice (i.e., Kim et al., 2010) can occur both in winter and spring, during massive ice melting. The enrichment of both Fe and Mn in the first 20 cm of the ice column relative to the deeper ice layers (**Fig. 5**) can certainly promote enhanced reductive dissolution of both Mn (Kim et al.,

2012) and Fe (Kim et al., 2010) under ice thaw during polar day in early June. However, Fe(II) fraction was estimated to be below 10% in June's lake sampling as the LMW$_{< 1\ \mathrm{kDa}}$ fraction containing essentially uncomplexed Fe^{2+}(aq) was ≤ 5% of total dissolved Fe (see method of Fe(II) analysis in the lake water by *in-situ* dialysis technique in Pokrovsky et al., 2012). Therefore, oxygenated spring waters and shallow depth of thermokarst lake provide favorable conditions of Fe(III) colloids formation in these organic-rich water bodies. Highly non-conservative behavior of DOC during the winter time demonstrating significant depletion in February **(Fig. 7 A)** may suggest some heterotrophic respiration of DOM under the ice. Alternatively, the DOC could be transformed into POC and precipitated to the lake bottom or be trapped as particles in the growing ice.

Note that the Zn concentration in winter become very high, up to 1 mg/L (Fig. 7 G). The main reason for such an increase of Zn concentration could be its high mobility in acidic, organic-rich aquatic systems. The additional mobilization of Zn from moss cover at the lake border during its freezing can be linked to the release of Zn from the cell cytoplasm during freeze-induced submerged vegetation cell damage. However that the concentration factor for Zn is not dramatically different from that of the other elements: it is similar to that of Cu, Zr, B, Na, K, REEs and U and even lower than that of Pb. As such we consider high element concentration during winter as being a consequence of solute concentration during freezing rather than specific mechanisms of metal mobilization from ground and bottom vegetation subjected to freezing.

During the massive ice melting, a significant number of coagulated organo-ferric particles remain on the ice surface (**Fig. S6**) and eventually precipitate to the lake bottom. Although under anaerobic conditions in the thermokarst lake sediments, Fe(III) may be reduced and return to the water column (Audry et al., 2011), the majority of Fe oxyhydroxide is likely to remain in the particulate form, thus preventing Fe to move to the hydrological network during spring floods. We hypothesize that one of the most powerful mechanisms of organic and organo-mineral colloid coagulation in thermokarst water bodies is annual freezing of the whole water column leading to significant concentration of Fe, C_{org} and related divalent metals and trivalent and tetravalent hydrolysates in the particulate phase. In the northern part of discontunuous permafrost zone, the lake sediments are indeed enriched in Fe and trivalent and and tetravelent hydrolysates (Audry et al., 2011). It is remarquable that Fe-normalized distribution coefficients of TE between the organo-ferric coagulates and filtered (< 0.45 µm) lake water (Fig. 8) are of the same order of magnitude or within a factor of 2 different from the distribution coefficients of TE between Fe-rich colloids (1 kDa – 0.45 µm) and $LMW_{< 1 \text{ kDa}}$ fraction assessed in previous studies in thermokarst lakes (Pokrovsky et al., 2013) and boreal surface streams (Vasyukova et al., 2010). This similarity strongly suggests that the elementary mechanisms of TE incorporation in organic matter-stabilized Fe oxyhydroxids include mainly co-precipitation and that it is generally similar for colloids and particles.

4.3. Allochthonous versus autochthonous processes forming lake water chemical composition

Allochthonous processes forming lake water chemical composition include the input of fresh vegetation products and the leaching of the upper peat layer. At the beginning of the active season, in June, there is a lateral input of melting snow, reflecting the interaction of water with ground vegetation such as mosses and lichens as well as with the litter fall of the dwarf shrubs from the previous year. During summer (baseflow) season, there is a peat leaching at the lake border via mainly wave abrasion and element and DOC release from moss and lichen coverage via lateral flow fed by rains.

The DOM entering the lake ecosystem with the snow melt and surface inflow during summer rain is subjected to two processes of autochthonous transformation during open water period: photo- and bio-degradation, mostly pronounced in June – September (i.e., Larouche et al., 2015). During summer, the productivity of phytoplankton including possible exometabolite release represents less than 10% of heterotrophic bacterioplankton respiration in western Siberian thermokarst lakes of the discontinuous/sporadic permafrost zone (Shirokova et al., 2013). The heterotrophic bacterioplankton activity brings about the conversion of colloidal DOM and low molecular weight (LMW) organic ligands to particulate organic matter (POM) in the form of coagulates or the bacterioplankton biomass; in both forms, the POM is likely to precipitate to the lake bottom in the course of the active season. During the glacial period, the processes leading to sedimentation of POC to the lake bottom are cryoconcentration and colloid coagulation (see Sect. 4.2 and Fig. S6). The physico-chemical coagulation of DOC may become especially important during progressive lake freezing in winter. Highly non-conservative behavior of DOC (Fig. 7a) relative to the other major components (Si, K, Na) strongly suggests the preferential removal of DOC from the remaining water under the ice cover. The other elements such as metals Fe, Ni, Cd and Pb (Fig. 7 c, i, k, l, respectively) follow non-conservative behavior of DOM suggesting their massive removal from the water column in the form of organic coagulates. In contrast, Al, Ti, Zn, Cr and Cu (Fig. 7 d, e, g, h, j, respectively) remain conservatively in the bottom water or even accumulated in the water. It is possible that they are less dependent on large-size DOM colloids mostly subjected to coagulation during cryoconcentration. Indeed, these metals could be bound to LMW$_{< 1\ \mathrm{kDa}}$ organic complexes and thus remain in unfrozen water in the lake bottom layer. Additional input of Al and Ti from mineral clayer sediments of the lake (i.e., Audry et al., 2011) cannot be excluded.

The behavior of DIC is almost conservative during lake freezing, without any excess of DIC over theoretical value in February. As a result, there is no significant accumulation of inorganic carbon in the form of CO_2 or HCO_3^- under the ice cover. This result strongly suggests the dominance of physico-chemical coagulation rather than microbial respiration in DOC removal from the water column in winter. The latter process dominates the open water period, when heterotrophic aerobic bacterioplankton respiration of allochthonous DOM produces gaseous CO_2 that is released to the atmosphere in western Siberia thermokarst lakes which are strongly supersaturated with respect to atmosphere (Shirokova et al., 2009, 2013), similar to the other boreal lakes (Jansson et al., 2008; Rautio et al., 2011). The response of this microbial process to the DOC input in the lake may be fast, on the matter of days, given that *i*) we observed elevated (> 20 mg/L) DOC concentration in smallest (< 2 m^2) ground depressions formed within hours after snowmelt, and *ii*) the leaching of DOM from plant litter is very fast, on the order of hours (Berg, 2000; Fraysse et al., 2010).

A plot of DOC concentration versus water residence time in medium and large lakes (300-1,200,000 m^2) revealed two clusters of the data points, with maximal DOC concentration observed in lakes and ponds of short-term water circulation and a stable and rather low DOC concentration (10 ± 5 mg/L) in lakes of slow water turnover (**Fig. 8a**). Since the allochthonous input increases DOC in the water body and autochthonous microbial respiration and physico-chemical coagulation remove DOC from the water column, the former process is certainly dominant for short-living water bodies. The hydrological balance of the smallest water depressions (< 200 m^2) could not be quantitatively assessed but it can be suggested that the lowest water residence time in these, partially ephemeral, water bodies is consistent with the highest DOC measured in this study. In the lakes of slow water turnover, the input and removal of DOC are presumably balanced. Note, however, the similarity of the intensity of autochthonous processes in larger lakes (i.e., ≥ 100,000 m^2), regardless of their size and the water residence time.

4.4. Seasonal evolution of stock of carbon and TE in thermokarst lakes

The average of the six smallest (< 1 m^2) depressions sampled in spring shows a factor of 2.3 ($p < 0.05$) higher concentration of dissolved organic carbon (30.8 ± 7.3 mg/L) compared to the larger water bodies (13.2±6.6 mg/L) during this period. This strongly suggests the importance of short-term plant debris (litter) and submerged ground vegetation leaching occurring right after the snowmelt. On the western Siberia lowland, the water stock is the highest during the spring period, notably in terms of water coverage of the land depressions (60 to 70% of the overall watershed area, Zakharova et al., 2014). According to satellite observations in western Siberia, the area subjected to the spring flood period is 55-65% higher than that of the summer period (Zakharova et al., 2014). Taking into account these observations, and the DOC concentration in thermokarst water bodies, we estimate that the overall increase of soluble stock of DOC and related metals in surface waters in June relative to August may be as high as 200 - 500%. This value stems from (*i*) a factor of 2 - 3 increase in the wetland flooding in June compared to summer baseflow season multiplied by (*ii*) a factor of 1.5 - 2 higher DOC and metal concentration in small (< 1-10 m^2) water bodies compared to the larger lakes. This dissolved fraction may be easily mobilized from the watershed to the river and further transported to the ocean.

In shallow thermokarst lakes, progressive ice melt from the surface towards the bottom slowly liberates inorganic carbon trapped or dissolved in the ice. The K_d(water/ice) for DIC (1.2-2.2) is much lower compared to other elements including DOC. As such, the ice is not particularly enriched in DIC relative to the bottom water and both winter and spring period DIC and CO_2 concentrations are not significantly higher than those in summer. At present, we do not know of any seasonal measurements of CO_2 and CH_4 in thermokarst water bodies of western Siberia. Our unpublished data (Figure S11 of Supplement) do not demonstrate any significant enrichment in CO_2 or CH_4 during spring flood. Only in very small depressions (< 10 m^2), the CO_2 level does increase. Given that the concentration of methane is 1 to 2 orders of magnitude lower than that of CO_2 and [CH_4] is independent on the depression size, the role of methane oxidation in CO_2 enrichment is negligible. Overall, we do not expect significant buildup of CO_2 under ice and CO_2 release from the lake water to the atmosphere during spring melt, contrasting to well known phenomena on deep boreal lakes (Karlsson et al., 2013). The reasons for this contrast could be low volume of the thermokarst lake water and relatively short period suitable for this accumulation in western Siberia, since already in February, there is a lack of liquid water under the ice, yielding a very low fraction (between 10 and 20%) of this unfrozen water stock. Altogether these arguments suggest that the only mechanism capable of enriching the lake water in CO_2 during spring melt is heterotrophic respiration of “fresh” allochthonous DOM, as confirmed by elevated DOC concentration during this period, notably in small water bodies.

Conclusions

A hydrochemical study of shallow thermokarst lakes from a discontinuous permafrost zone of western Siberia revealed conceptually new features of element concentration evolution over different seasons within a large scale of the lake size. Statistical treatment demonstrated that there is no significant difference in element concentration as a function of the lake size within the range of $2 \cdot 10^2 – 2 \cdot 10^6$ m² in June, August and October. However, in spring, there was a clear increase of DOC and related metal concentration with the decrease in the size of small water bodies (< 200 m²). Such small ponds disappear in summer due to evaporation and quickly freeze solid at the very beginning of the glacial season. Most of the dissolved elements and organic carbon decreased their concentration following the order June < August < October, regardless of the lake size range, from $2 \cdot 10^2$ to $2 \cdot 10^6$ m². Therefore, although there are statistically significant differences in organic carbon, major and trace element concentration between different seasons, the lake size has a negligible influence on the lake water chemical composition, except in very small water bodies sampled only in spring. The water residence time (WRT) may be important parameter controlling lake DOC and Fe concentrations, especially for short – lived water bodies, mostly present during spring. In contrast, the other major and trace elements did not demonstrate any clear link with WRT in the lake.

The ice formation in October created an excessive pressure within the confined water body; the remaining organic- and Fe-rich water was seeping onto the ice surface via cracks of the ice cover. This seeping produced the ice of multiple layers with significant enrichment in Fe, DOC and trace elements in the frozen water pockets within the first 0-20 cm in depth. Massive coagulation of organo-ferric colloids occurred during full freezing of the lake water and produced macroscopic, organic- and Fe-rich amorphous particles capable to precipitate to the lake bottom. The main mechanisms of element differentiation during ice formation are concentration and coagulation of organic and organo-mineral colloids, as shown by highly non-conservative behavior of DOC and related metals. The partitioning coefficients of TE between the lake water (< 0.45 µm) and the particulate coagulates reflecting the degree of element differentiation during ice formation and full water column freezing were similar to those measured for Fe-rich colloids (1 kDa – 0.45 µm) in other thermokarst and boreal lakes and rivers.

The spring flood period created the highest stock of dissolved allochthonous DOC and related metals, notably in small (< 200 m²) water bodies and depressions. The water dilution during this period (e.g., typically 20% of the water volume increase) can compete with the increase in the land surface coverage for the overal element stock in lakes in June relative to August. We estimate that the overall increase of soluble stock of DOC and related metals in surface waters and consequently, potential for river water feeding by lakes during spring floods, ranged between a factor of 2 to 5. Further assessment of this increase requires high-resolution (< 0.5-1 m²) remote sensing observation coupled with *in-situ* hydrochemical measurements. Given significant coverage of the land surface by thaw water in spring and elevated DOC concentrations during this period, the overall impact of snowmelt on CO_2 emission into the atmosphere may be significantly higher compared to that in summer. In contrast, winter time period leading to full freezing of the water column is unlikely to build up significant GHG concentration under the ice and appreciably affect gas regime of thermokarst lakes at the annual scale.

Acknowledgements

This work was supported by BIO-GEO-CLIM grant No 14.B25.31.0001 of Russian Ministry of Science and Education and Tomsk State University, ANR CESA "Arctic Metals", RFBR 14-05-31457 mol_a and grant MK-3684.2015.5. We thank two anonymous reviewers for their constructive comments.

Author Contribution

RM performed sampling, analysis of major cations and trace elements, interpretation and statistical treatment; SV and S Kirpotin were responsible for the choice of sampling objects and logistics and statistical treatment; IK was the leader of winter sampling campaign and interpretation of lake freezing results; SL and S Kulizhsky provided the background information on soil, peat, and contributed to design and interpretation of summer, autumn and winter sampling campaigns; LS was in charge of DOC, DIC and anion measurements and their interpretation; V Shevchenko provided the expertise and practical performance of ice core sampling, handling and analyses; LK provided GIS-based interpretation, mapping and identification of sampled water bodies; VZ and V Sinkinov performed all primary hydrological data collection, their analysis and interpretation; OP and S Kirpotin provided supervision and placing this work in the context of current knowledge of western Siberia thermokarst lakes. All 12 authors spent significant amount of time in the field of Khanymey and Nojabrsk test sites. Each co-author have seen and approved the final paper and contributed to writing the manuscript.

REFERENCES

Audry, S., Pokrovsky, O. S., Shirokova, L. S., Kirpotin, S. N., and Dupré B.: Organic matter mineralization and trace element post-depositional redistribution in Western Siberia thermokarst lake sediments, Biogeosciences, 8, 3341–3358, 2011.

Avagyan, A., Runkle, B.R.K., Kutzbach, L.: Application of high-resolution spectral absorbance measurements to determine dissolved organic carbon concentration in remote areas, J. Hydrology 517, 435–446, 2014.

Benedetti, M.F., Milne, C., Kinniburgh, D., van Riemsdijk, W., Koopal, L.: Metal ion binding to humic substances: Application of the non ideal competitive adsorption model, Environ. Sci. Technol. 29, 446-457, 1995.

Berg, B.: Litter decomposition and organic matter turnover in northern forest soils, Forest Ecol. Manag. 133, 13-22, 2000.

Boike, J., Kattenstroth, B., Abramova, K., Bornemann, N., Chetverova, A., Fedorova, I., Fröb, K., Grigoriev, M., Grüber, M., Kutzbach, L., Langer, M., Minke, M., Muster, S., Piel, K., Pfeiffer, E.-M., Stoof, G., Westermann, S., Wischnewski, K., Wille, C., and Hubberten, H.-W.: Baseline characteristics of climate, permafrost and land cover from a new permafrost observatory in the Lena River Delta, Siberia (1998–2011), Biogeosciences, 10, 2105-2128, 2013.

Bouchard, F., Francus, P., Pienitz, R., Laurion, I., Feyte, S. : Subarctic thermokarst ponds : investigating recent landscape evolution and sediment dynamics in thawed permafrost of Northern Québec (Canada), Arctic, Antarctic and Alpine Res., 46(1), 251-271.

Dillon, P.J., Molot, L.A.: Dissolved organic and inorganic carbon mass balances in central Ontario lakes. Biogeochemistry, 36, 29-42, 1997.

Fraysse, F., Pokrovsky, O. S., and Meunier, J.-D.: Experimental study of terrestrial plant litter interaction with aqueous solutions, Geochim. Cosmochim. Ac., 74, 70–84, 2010.

Frey, K.E., Smith, L.C.: Amplified carbon release from vast West Siberian peatlands by 2100, Geophys. Res. Letters 32, L09401, doi: 10.1029/2004GL022025, 2005.

Frey, K.E., Siegel, D.I., Smith, L.C.: Geochemistry of west Siberian streams and their potential response to permafrost degradation, Water Resources Res. 43, W03406, doi: 10.1029/2006WR004902, 2007.

Grosse, G., Jones, B., Arp, C.: Thermokarst lakes, drainage, and drained basins. In: Shroder, J. (Editor in Chief), Giardino, R., Harbor, J. (Eds.), Treatise on Geomorphology. Academic Press, San Diego, CA, vol. 8, Glacial and Periglacial Geomorphology, pp. 325-353, 2013.

Gustafsson, J.: WinHumicV for Win95/98/NT, 1999. http://amov.ce.kth.se/people/gustafjp/winhumicv.htm. A Windows version of MINTEQA2 website, Gustafsson, J.; http://www.lwr.kth.se/English /OurSoftware/vminteq/index.htm, 1999.

Jansson, M., Hickler, Th., Jonsson, A., Karlsson, J.: Links between terrestrial primary production and bacterial production and respiration in lakes in a climate gradient in subarctic Sweden. Ecosystems 11, 367-376, 2008.

Karlsson, J., Giesler, R., Persson, J., and Lundin, E.: High emission of carbon dioxide and methane during ice thaw in high latitude lakes, Geophysical Research Letters, 40(6), 1123-1127, 2013.

Karlsson, J.M., Lyon, S.W., Destouni, G. : Thermokast lake, hydrological flow and water balance indicators of permafrost change in Western Siberia, J. Hydrol., 464-465, 459-466, 2012.

Karlsson, J.M., Lyon, S.W., and Destouni, G.: Temporal behavior of lake size-distribution in a thawing permafrost landscape in Northwestern Siberia, Remote Sens., 6(1), 621-636, 2014.

Kim, K., Choi, W., Hoffmann, M. R., Yoon, H.-I., and Park, B.-K.: Photoreductive dissolution of iron oxides trapped in ice and its environmental implications, Environ. Sci. Technol., 44, 4142-4148, 2010.

Kim, K., Yoon, H.-I., and Choi, W.: Enhanced dissolution of manganese oxide in ice compared to aqueous phase under illuminated and dark conditions, Environ. Sci. Technol., 46, 13160-13166, 2012.

Kirpotin, S.N., Polishchuk, Y.M., Zakharova, E., Shirokova, L., Pokrovsky, O., Kolmakova, M., Dupré, B.: One of possible mechanisms of thermokarst lakes drainage in West-Siberian North. International Journal of Environmental Studies, 65, No 5, 631-635, 2008.

Larouche, J.R., Abbott, B.W., Bowden, W.B., Jones, J.B.: The role of watershed characteristics, permafrost thaw, and wildfire on dissolved organic carbon biodegradability and water chemistry in Arctic headwater streams, Biogeosciences Discuss., 12, 4021-4056, 2015.

Laurion, I., Vincent, W. F., MacIntyre, S., Retamal, L., Dupont, C., Francus, P., and Pienitz, R.: Variability in greenhouse gas emissions from permafrost thaw ponds, Limnol. Oceanogr., 55, 115-133, 2010.

Manasypov, R. M., Pokrovsky, O. S., Kirpotin, S. N., and Shirokova, L. S.: Thermokarst lake waters across the permafrost zones of western Siberia, The Cryosphere, 8, 1177-1193, 2014.

Milne, C.J., Kinniburgh, D.G., van Riemsdijk, W.H., Tipping, E.: Generic NICA-donnan model parameters for metal-ion binding by humic substances, Environ. Sci. Technol. 37(5), 958-971, 2003.

Muller, S., Vahatalo, A. V., Stedmon, C. A., Granskog, M. A., Norman, L., Aslam, S., Underwood, G.J.C., Dieckmann, G.S., and Thomas, D.N.: Selective incorporation of dissolved organic matter (DOM) during sea ice formation, Mar. Chem., 155, 148-157, 2013.

Novikov, S.M.: Hydrology of Bog Territories of the Permafrost Zone of Western Siberia. St Petersbourg, BBM Publ. House, 536 pp, in Russian (ISBN 978-5-9651-0339-3), 2009.

Negandhi, K., Laurion, I., Whiticar, M.J., Galand, P.E., Xu, X., and Lovejoy, C.: Small thaw ponds: An accounted source of methane in the Canadian high Arctic, Plos One, 8(11), e78204, 2013.

Pokrovsky, O. S., Shirokova, L. S., Kirpotin, S. N., Audry, S., Viers, J., and Dupré, B.: Effect of permafrost thawing on organic carbon and trace element colloidal speciation in the thermokarst lakes of western Siberia, Biogeosciences, 8, 565–583, 2011.

Pokrovsky, O.S., Shirokova, L. S., Zabelina, S. A., Vorobieva, T. Y, Moreva, O. Y., Klimov, S. I., Chupakov, A. V., Shorina, N. V., Kokryatskaya, N. M., Audry, S., Viers, J., Zouite, C., Freydier, R.: Size fractionation of trace elements in a seasonally stratified boreal lake: control of organic matter and iron colloids, Aquatic Geochemistry, 18, 115–139, 2012.

Pokrovsky, O. S., Shirokova, L. S., Kirpotin, S. N., Kulizhsky, S. P., and Vorobiev, S. N.: Impact of western Siberia heat wave 2012 on greenhouse gases and trace metal concentration in thaw lakes of discontinuous permafrost zone, Biogeosciences, 10, 5349-5365, 2013.

Pokrovsky, O.S., Shirokova, L.S., and Kirpotin, S.N.: Biogeochemistry of Thermokarst Lakes of Western Siberia, Nova Science Publ. Inc., N. Y., 163 pp., 2014.

Rautio, M., Dufresne, F., Laurion, I., Bonilla, S., Vincent, W. F., and Christoffersen, K.: Shallow freshwater ecosystems of the circumpolar Arctic, Ecoscience, 18, 204-222, 2011.

Shirokova, L. S., Pokrovsky, O. S., Kirpotin, S. N., and Dupré, B.: Heterotrophic bacterio-plankton in thawed lakes of the northern part of Western Siberia controls the CO_2 flux to the atmosphere, Int. J. Environ. Stud., 66, 433–445, 2009.

Shirokova, L. S., Pokrovsky, O. S., Viers, J., Klimov, S. I., Moreva, O. Yu., Zabelina, S. A., Vorobieva, T. Ya., and Dupré, B.: Diurnal variations of trace metals and heterotrophic bacterioplankton concentration in a small boreal lake of the White Sea basin, Ann. Limnol.-Int. J. Lim., 46, 67-75, 2010.

Shirokova, L. S., Pokrovsky, O. S., Kirpotin, S. N., Desmukh, C., Pokrovsky, B. G., Audry, S., and Viers, J.: Biogeochemistry of organic carbon, CO_2, CH_4, and trace elements in thermokarst water bodies in discontinuous permafrost zones of Western Siberia, Biogeochemistry, 113, 573–593, 2013.

Stepanova, V.M., Pokrovsky, O.S., Viers, J., Mironycheva-Tokareva, N.P. Kosykh, N.P., Vishnyakova, E.K.: Major and trace elements in peat profiles in Western Siberia: impact of the landscape context, latitude and permafrost coverage, Applied Geochemistry, 53, 53–70, 2015.

Tank, S.E., Lesack, L.F.W., Gareis, J.A.L., Osburn, C.L., and Hesslein, R.H.: Multiple tracers demonstrate distinct sources of dissolved organic matter to lakes of the Mackenzie Delta, western Canadian Arctic, Limnol. Oceanogr., 56(4), 1297–1309, 2011.

Tank, S.E., Esslein, R.H.H., and Esack, L.F.W.L.: Northern delta lakes as summertime CO_2 absorbers within the arctic landscape, Ecosystems, 12, 144–157, 2009.

Unsworth, E.R., Warnken, K.W., Zhang, H., Davison, W., Black, F. et al.: Model predictions of metal speciation in freshwaters compared to measurements by in situ techniques, Environ. Sci. Technol. 40 (6), 1942-1949, 2006.

Vasyukova, E. V., Pokrovsky, O. S., Viers, J., Oliva, P., Dupré, B., Martin, F., and Candaudap, F.: Trace elements in organic- and iron-rich surficial fluids of the boreal zone: Assessing colloidal forms via dialysis and ultrafiltration, Geochim. Cosmochim. Ac., 74, 449–468, 2010.

Walter, K. M., Zimov, S. A., Chanton, J. P., Verbyla, D., and Chapin, F. S.III.: Methane bubbling from Siberian thaw lakes as a positive feedback to climate warming, Nature, 443, 71-75, 2006.

Walter, K. M., Chanton, J. P., Chapin III, F. S., Schuur, E.A.G., and Zimov, S.A.: Methane production and bubble emissions from arctic lakes: Isotopic implications for source pathways and ages, J. Geophys. Res, 113, G00A08, 2008.

Walter Anthony, K.M., Anthony, P., Grosse, G., and Chanton, J.: Geologic methane seeps along boundaries of Arctic permafrost thaw and melting glaciers, Nature Geoscience, 5, 419–426, 2012.

Walter Anthony, K. M. and Anthony, P.: Constraining spatial variability of methane ebullition in thermokarst lakes using point-process models, J. Geophys. Res, 118, doi:10.1002/jgrg.20087, 2013.

Walter Anthony, K. M., Zimov, S. A., Grosse, G., Jones, M. C., Anthony, P. M., Chapin III, F. S., Finlay, J. C., Mack, M. C., Davydov, S., Frenzel, P., and Frolking, S.: A shift of thermokarst lakes from carbon sources to sinks during the Holocene epoch, Nature, 511, 452-456, 2014.

Weishaar, J.L., Aiken, G.R., Bergamaschi, B.A., Fram, M.S., Fujii, R., Mopper, K.: Evaluation of specific ultraviolet absorbance as an indicator of the chemical composition and reactivity of dissolved organic carbon, Environ. Sci. Technol. 37, 4702–4708, 2003.

Yeghicheyan, D., Bossy, C., Bouhnik Le Coz, M., Douchet, C., Granier, G., Heimburger, A., Lacan, F., Lanzanova, A., Rousseau, T. C. C., Seidel, J.-L., Tharaud, M., Candaudap F., Chmeleff, J., Cloquet, C., Delpoux, S., Labatut, M., Losno, R., Pradoux, C., Sivryn Y., and Sonke, J. E.: A Compilation of silicon, rare earth element and twenty-one other trace element concentrations in the natural river water reference material SLRS-5 (NRC-CNRC), Geostand. Geoanal. Res., 37, 449-467, 2014.

Zakharova, E. A., Kouraev, A. V., Kolmakova, M. V., Mognard, N. M., Zemtsov, V. A., and Kirpotin, S. N.: The modern hydrological regime of the northern part of Western Siberia from in situ and satellite observations, Int. J. Environ. Stud., 66, 447-463, 2009.

Zakharova, E. A., Kouraev, A. V., Frédérique R., Zemtsov, V. A., Kirpotin S. N., Seasonal variability of the Western Siberia wetlands from satellite radar altimetry, J. Hydrol., 512, 366-378, 2014.

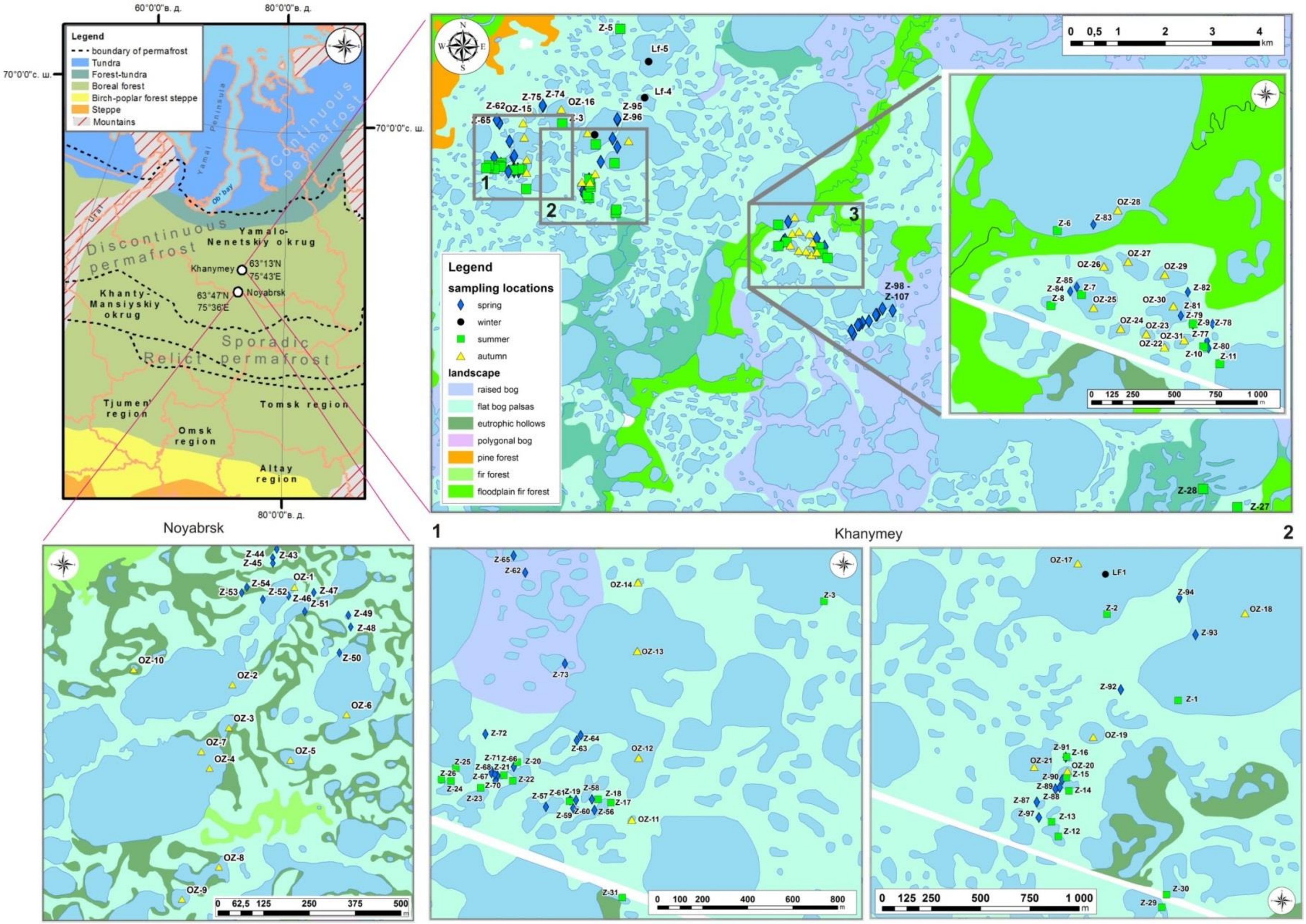

Figure 1. Study site area with symbols showing the position of sampled lakes and small water bodies in different seasons. Different colors correspond to different elementary ecosystems.

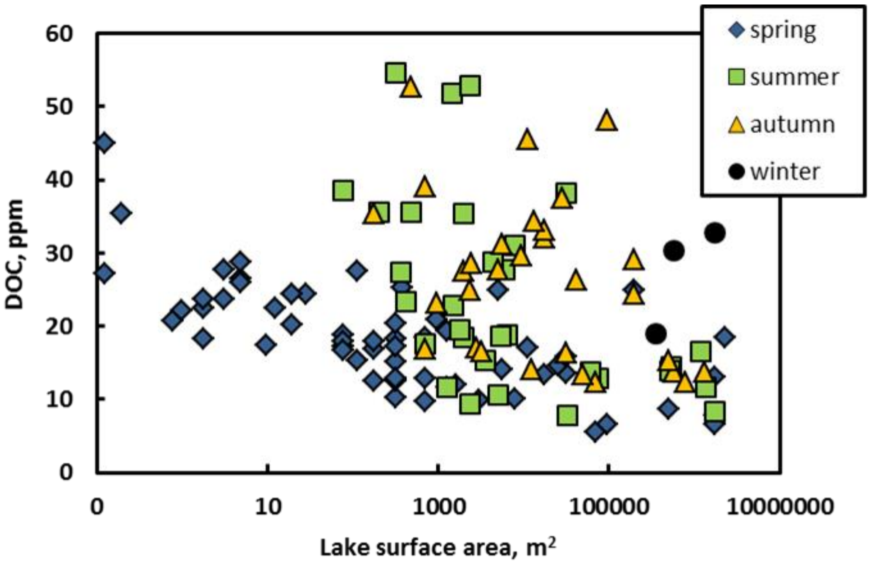

Figure 2. DOC concentration in thermokarst lakes of various size during 4 observation seasons.

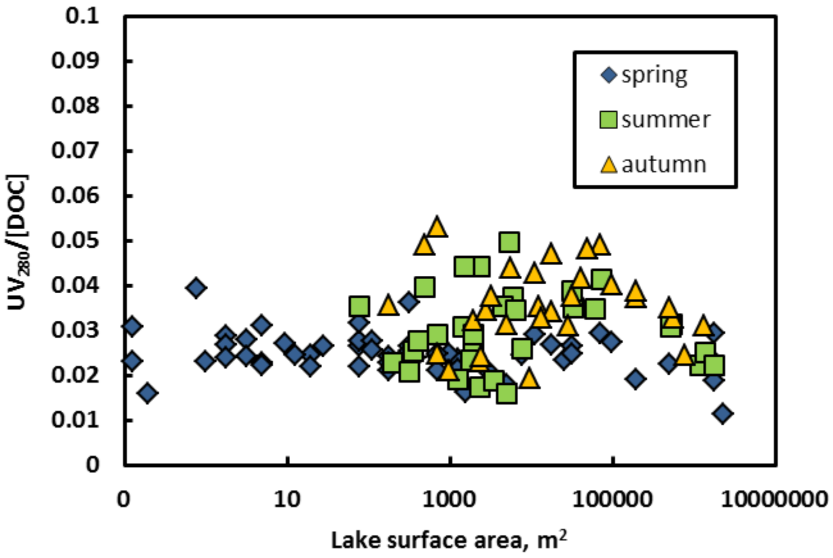

Figure 3. UV absorbence properties of thermokarst lake waters. The UV$_{280}$ /DOC ratio increases in the order spring < summer < autumn suggesting the progressive increase of aromaticity which is independent on the lake size ($p > 0.05$). The average values of UV$_{280\ nm}$/|DOC] are equal to 0.024±0.0037, 0.030±0.0072, 0.035±0.0069, and 0.0354±0.0068 cm^{-1} in spring, summer, autumn and winter, respectively.

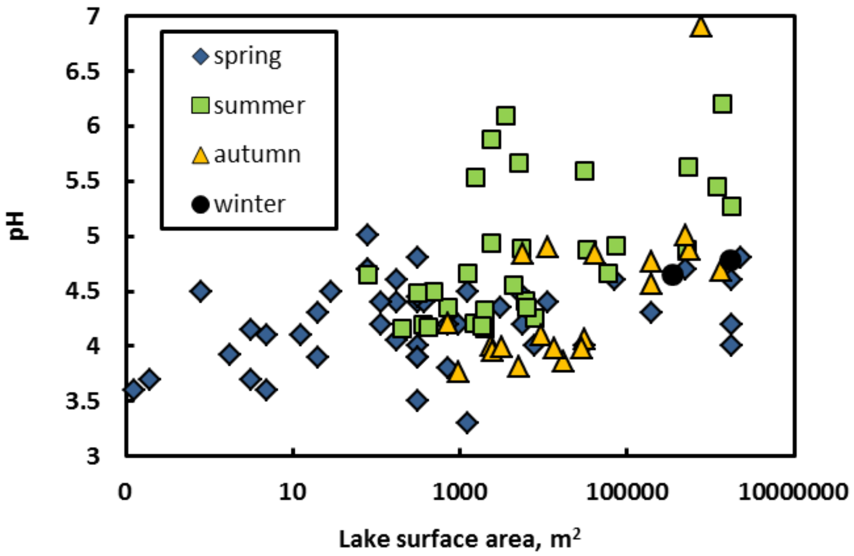

Figure 4. Increase of lake water pH with the increase of the lake size over 4 studied season. Note that the lowest pH is observed in spring and the highest in summer. This likely reflects the dominance of allochthonous organic input in the lake in spring, notably in the smallest water bodies, and autochthonous processes of some phytoplankton and macrophytes activity in the end of the summer.

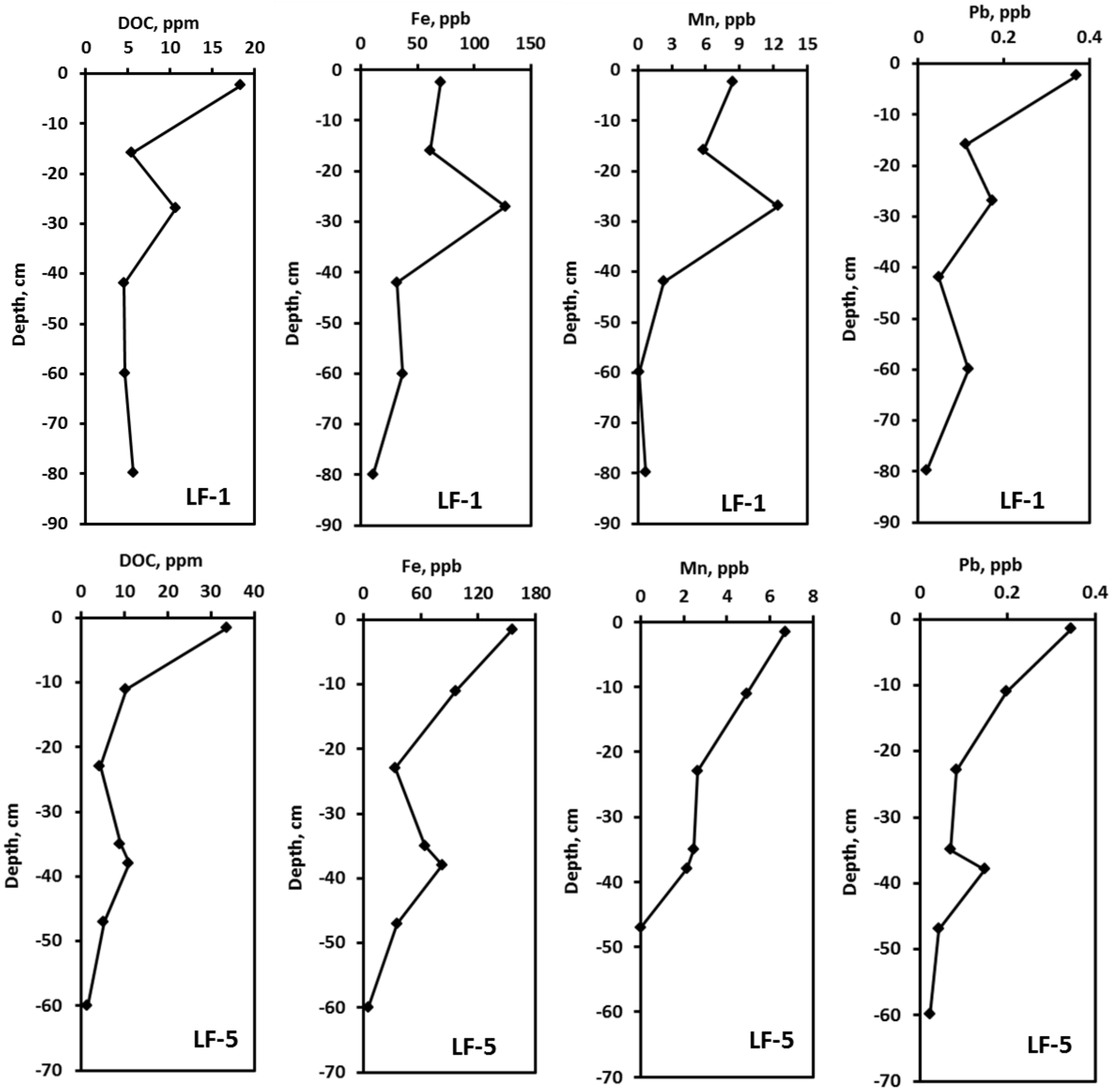

Figure 5. DOC, Fe, Mn and Pb concentration in the ice cores of thermokarst lakes sampled in February 2014. LF-1 and LF-5 refer to sampled lakes (Table 1).

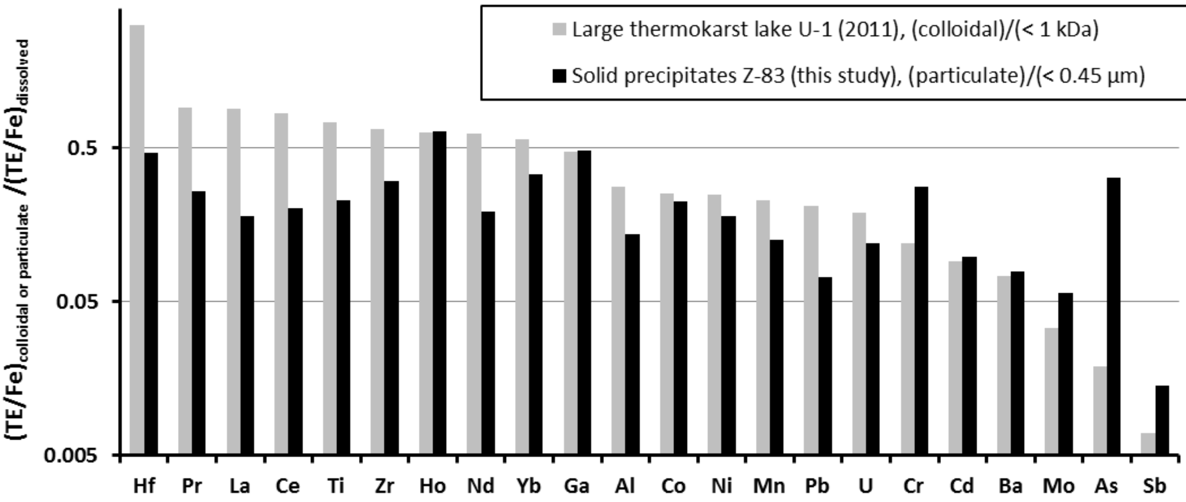

Figure 6. Comparison of the distribution coefficients of trace element (TE) normalized to Fe between the solid precipitates collected in June from the ice surface of large lake (Fig. S6) and filtered water (black columns) and those measured between colloids (1 kDa – 0.45 µm) and LMW$_{< 1\ \mathrm{kDa}}$ fraction in large thermokarst lake (Pokrovsky et al., 2011) of discontinuous permafrost zone (grey columns).

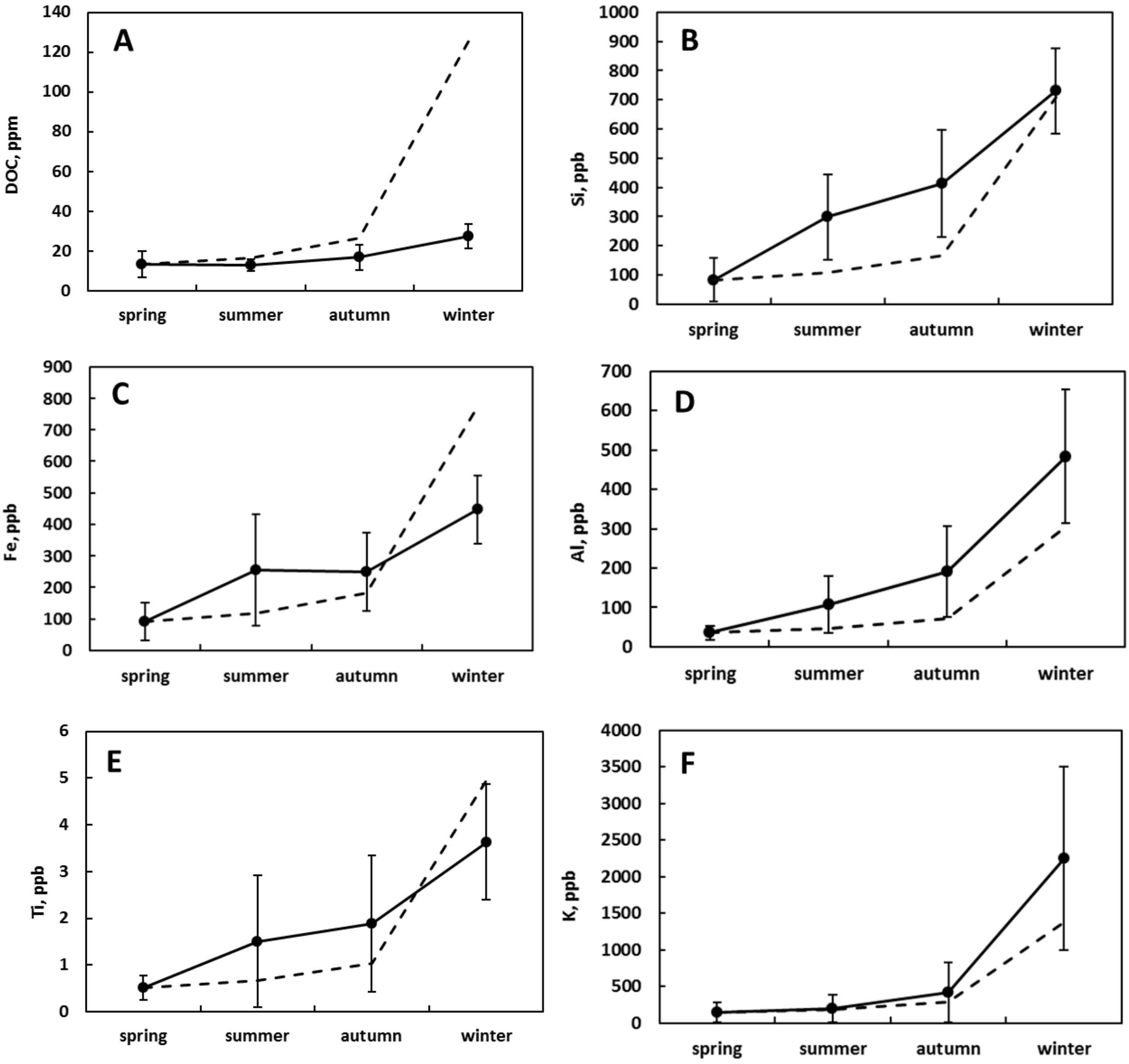

Figure 7. Size-averaged concentration of DOC (A), Si (B), Fe (C), Al (D), Ti (E), K (F), Zn (G), Cr (H), Ni (I), Cu (J), Cd (K) and Pb (L) during different seasons. The points are the average and the error bars are the standard deviation. Only the medium and large lakes (> 100 m² surface area) were used for this estimation. The dotted line represents conservative behavior for a hypothetical lake of 75 cm depth in summer, 20 cm flooding in spring, surface 20 cm ice formation in October, and almost full freezing (10 cm bottom water left) in February.

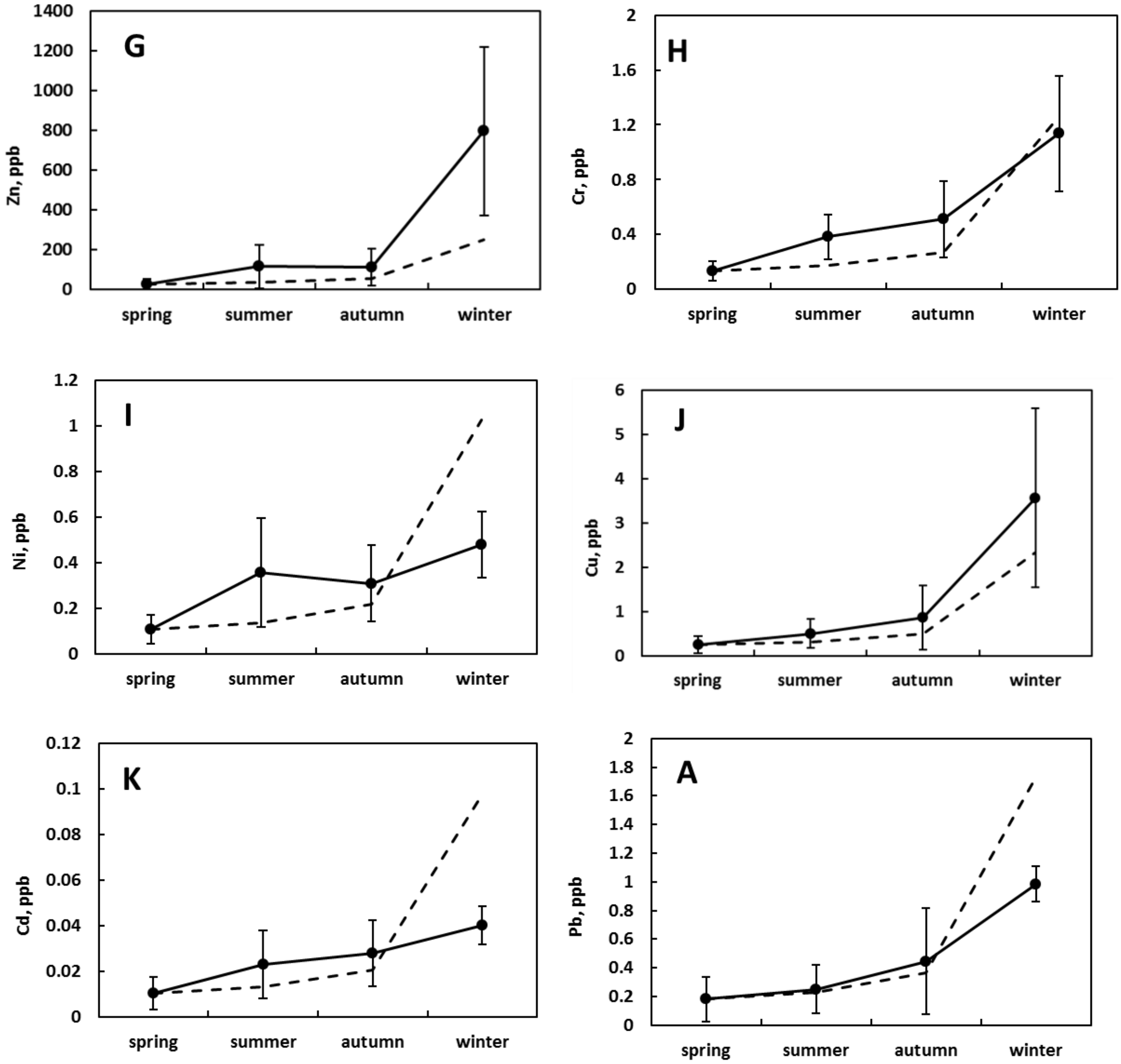

Figure 7, continued.

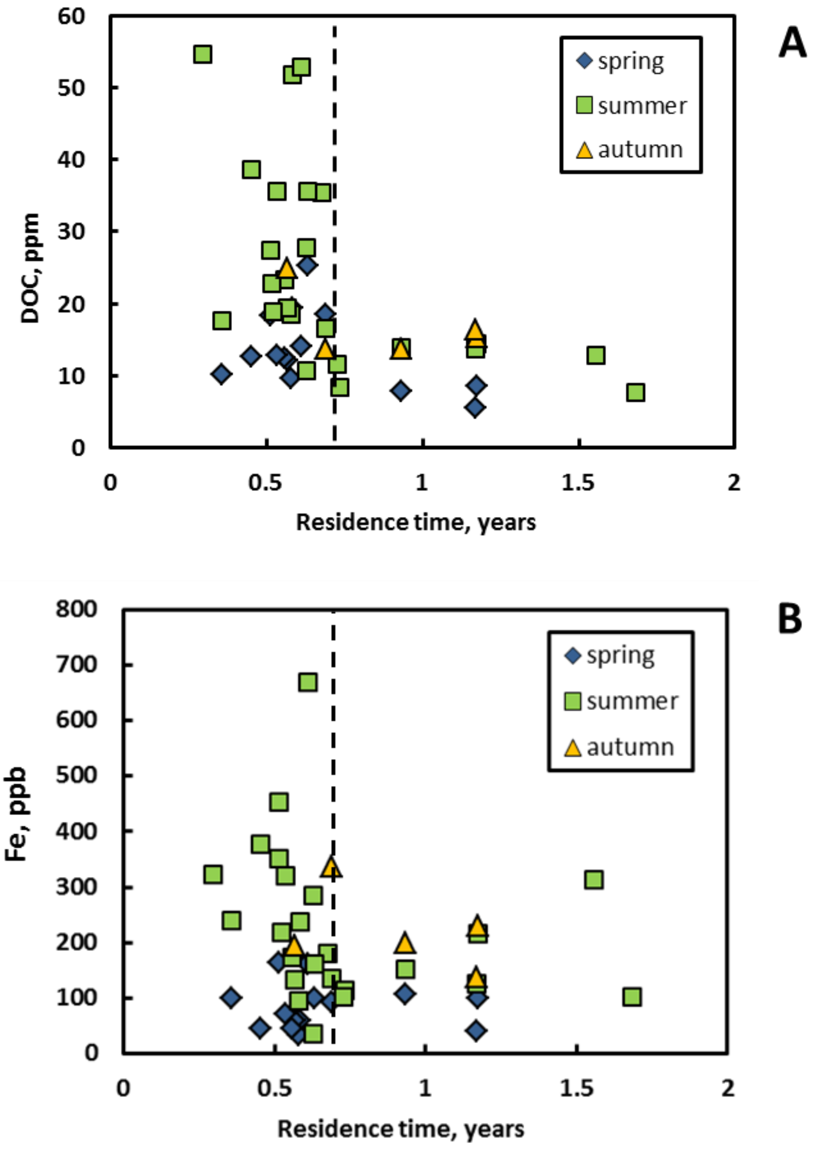

Figure 8. DOC (A) and Fe (B) concentration during different seasons plotted as a function of water residence time in the water body.

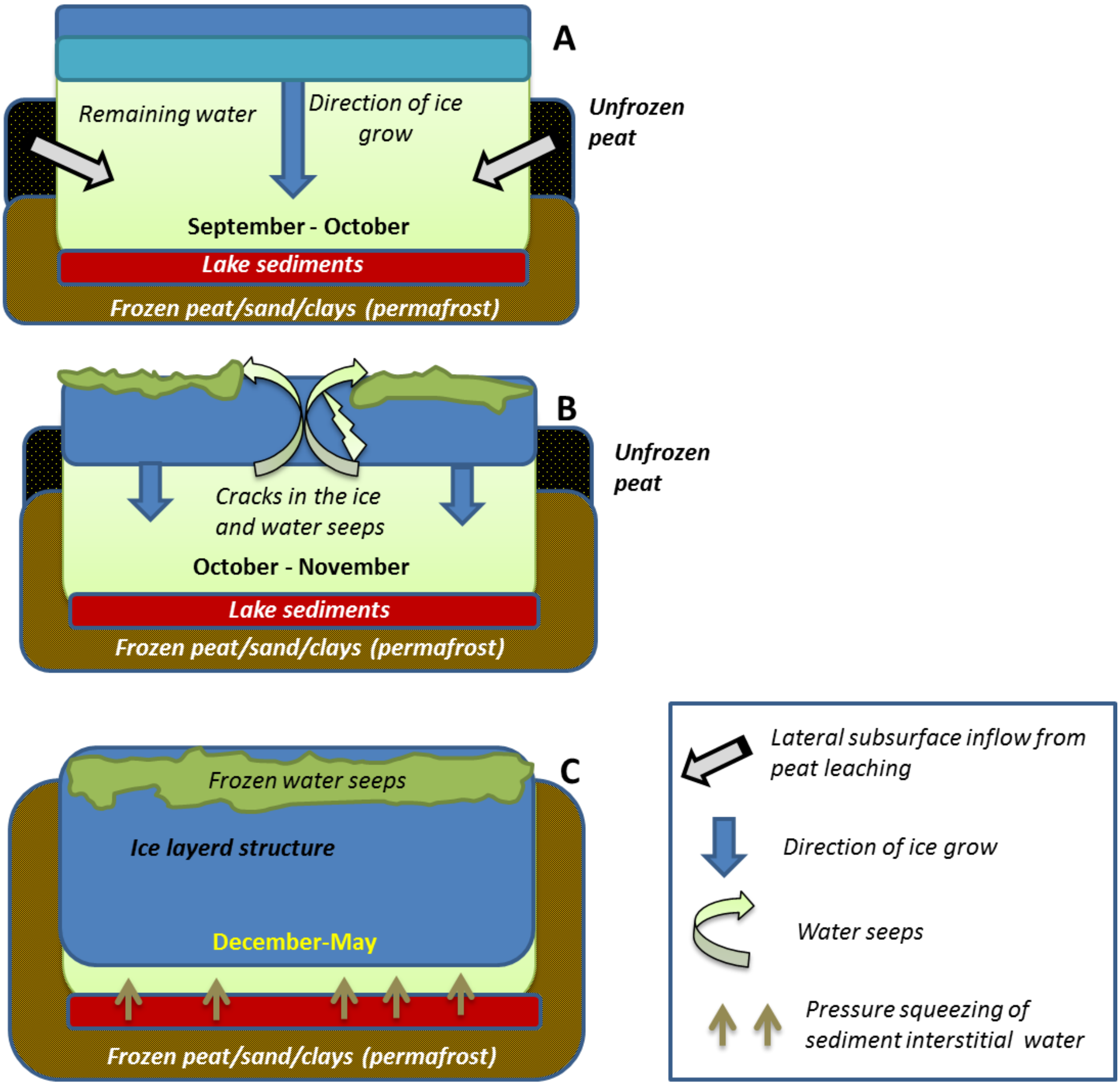

Figure 9. Sequence of ice crystallization events during the glacial period on the shallow (< 1 m depth) thermokarst lakes of western Siberia. A: start of the ice formation; B: squeezing water towards the surface via seeps; C: freezing of water pockets and seeps and multi-layer ice formation.

Table 1. Major hydrophysical and hydrochemical parameters of studied lakes.

	N	E	S, m^2	T, ^{o}C	O_2, mg/L	O_2, % sat	R, µS cm^{-1}	pH	DIC, ppm	DOC, ppm	Cl, ppm	SO_4, ppm
June												
Z-43	63°13,580'	75°43,476'	**1.8**	6.5	N.D.	N.D.	N.D.	3.43	0.749	22.5	0.1532	0.9452
Z-44	63°13,567'	75°43,465'	**0.071**	7.5	N.D.	N.D.	N.D.	3.25	0.562	33.9	0.1458	0.9957
Z-45	63°13,559'	75°43,467'	**4.9**	6.0	N.D.	N.D.	N.D.	3.43	0.784	26.5	0.1466	0.8256
Z-46	63°13,513'	75°43,527'	**31400**	7.2	N.D.	N.D.	N.D.	3.28	0.396	13.6	0.0663	0.3680
Z-47	63°13,521'	75°43,608'	**1.8**	5.5	N.D.	N.D.	N.D.	3.51	0.598	23.6	0.0978	0.5896
Z-48	63°13,492'	75°43,726'	**78.5**	5.9	N.D.	N.D.	N.D.	3.49	0.433	17.2	0.0306	0.4516
Z-49	63°13,475'	75°43,737'	**1.0**	5.2	N.D.	N.D.	N.D.	3.37	0.545	22.1	0.1285	0.7087
Z-50	63°13,436'	75°43,707'	**96163**	7.5	N.D.	N.D.	N.D.	3.77	0.550	6.5	0.0848	0.4372
Z-51	63°13,492'	75°43,584'	**25434**	7.2	N.D.	N.D.	N.D.	3.08	0.435	14.7	0.0131	0.448
Z-52	63°13, 505'	75°43,444'	**17663**	6.6	N.D.	N.D.	N.D.	3.36	0.390	13.3	0.0678	0.369
Z-53	63°13,512'	75°43,374'	**9.6**	5.8	N.D.	N.D.	N.D.	3.47	0.447	17.4	0.0289	0.576
Z-54	63°13,521'	75°43,389'	**0.13**	5.5	N.D.	N.D.	N.D.	3.11	0.855	27.2	0.1337	0.752
Z-56	63°47'55,0"	75°31'21,0"	**5671.6**	3.8	9.1	86	12	4.2	0.431	14.1	0.1781	0.097
Z-57	63°47'54,4"	75°31'6,55"	**3000**	5.7	8.86	82	12	4.35	0.423	9.8	0.1637	0.616
Z-58	63°47'56,5"	75°31'19,9"	**314**	6.2	8.19	79	13	4.4	0.438	10.2	0.1616	0.595
Z-59	63°47'56,2"	75°31'14,8"	**5024**	6.0	8.3	77	30	4.5	0.437	24.9	0.0501	0.476
Z-60	63°47'55,0"	75°31'14,1"	**314.0**	6.6	8.23	78	21	4.0	0.459	15.2	0.0657	0.301
Z-61	63°47'56,1"	75°31'12,9"	**176.6**	6.5	8.2	77	17	4.05	0.410	12.5	0.0809	0.589
Z-62	63°48'28,0"	75°30'52,1"	**1766250**	5.9	8.25	79	12	4.2	0.477	13.0	0.2440	0.843
Z-63	63°48'04,7"	75°31'13,4"	**28.3**	8.5	7.33	74	20	4.5	0.394	24.5	0.024	0.233
Z-64	63°48'05,0"	75°31'14,5"	**19.6**	10.5	8.54	88	23	4.3	0.524	24.4	0.040	0.615
Z-65	63°48'29,5"	75°30'50,5"	**11304**	8.3	8.6	86	14	4.4	0.449	17.1	0.157	0.731
Z-66	63°48'00,2"	75°30'53,8"	**314.0**	9.9	8.55	85	15	4.8	0.429	12.6	0.064	0.964
Z-67	63°47'59,3"	75°30'46,8"	**78.5**	11.4	8.38	90	28	5.01	0.402	18.8	0.050	0.385
Z-68	63°47'59,0"	75°30'46,8"	**176.6**	10.2	8.46	88	22	4.4	0.378	16.9	0.043	0.725

Asterisk stands for lake sampled during all four seasons

Table 1, continued.

	N	E	S, m^2	T, °C	O_2, mg/L	O_2, % sat	R, μS cm^{-1}	pH	DIC, ppm	DOC, ppm	Cl, ppm	SO_4, ppm
Z-69	63°47'58,7"	75°30'48,8"	**314.0**	8.5	9.2	99	14	3.9	0.458	12.9	0.149	0.341
Z-70	63°47'58,0"	75°30'48,3"	**78.5**	12.5	8.25	91	18	4.7	0.378	17.9	0.040	0.505
Z-71	63°47'58,9"	75°30'47,9"	**0.0079**	N.D.	N.D.	N.D.	N.D.	N.D.	0.610	22.6	1.484	0.843
Z-72	63°48'04,5"	75°30'43,7"	**1.8**	16.5	7.5	84	30	3.92	0.390	18.2	0.170	0.860
Z-73	63°48'15,5"	75°31'07,4"	**706.5**	12.9	8.7	98	17	3.8	0.372	12.8	0.069	0.339
Z-74(A)**	63°48'39,7"	75°31'59,9"	**503000**	6.3	9.2	94	9	4.0	0.426	7.8	0.146	0.647
Z-75	63°48'39,9"	75°31'59,4"	**0.20**	17.2	8.1	82	34	3.7	0.854	35.4	0.102	0.776
Z-77	63°46'58,0"	75°39'12,2"	**113**	12.4	7.95	87	32	4.4	0.432	27.5	0.102	0.247
Z-78	63°47'01,4"	75°39'14,0"	**3.1**	10.8	7.12	77	41	3.7	0.419	27.7	0.037	0.419
Z-79	63°47'01,0"	75°39'05,4"	**314**	12.7	7.6	86	18	3.5	0.304	18.3	0.022	0.201
Z-80	63°46'56,6"	75°39'13,1"	**1256**	11.8	7.8	85	23	3.3	0.303	19.4	0.093	0.276
Z-81	63°47'01,7"	75°39'02,2"	**31400**	12	8.3	93	19	4.0	0.323	15.8	0.304	0.163
Z-82	63°47'07,2"	75°39'02,0"	**113**	14.4	8.4	97	19	4.2	0.359	15.3	0.009	0.216
Z-83(B)**	63°47'18,9"	75°38'30,1"	**1396000**	3.4	8.6	82	11	4.6	0.858	6.5	0.117	0.209
Z-84	63°47'06,7"	75°38'10,8"	**314**	15.1	7.8	90	19	3.9	0.355	17.2	0.009	0.244
Z-85(C)**	63°47'05,4"	75°38'10,4"	**53630**	10.9	7.99	80	7	4.6	0.433	5.5	0.067	0.471
Z-87	63°47'41,5"	75°33'01,0"	**1256**	13.7	8.43	95	12	4.5	0.338	11.6	0.060	0.493
Z-88	63°47'43,9"	75°33'07,5"	**177**	20.5	8.02	98	N.D.	4.6	0.325	17.9	0.031	0.260
Z-89	63°47'44,2"	75°33'09,0"	**707**	N.D.	7.4	98	N.D.	N.D.	0.285	9.7	0.189	0.215
Z-90(D)**	63°47'45,5"	75°33'09,7"	**3485**	N.D.	7.9	95	N.D.	N.D.	0.283	12.1	0.138	0.146
Z-91	63°47'49,2"	75°33'10,3"	**380**	N.D.	7.8	95	23	4.4	0.329	25.3	0.045	0.247
Z-92	63°48'01,0"	75°33'28,5"	**78.5**	20	7.7	95	12	4.7	0.334	16.6	0.014	0.255
Z-93(E)**	63°48'11,0"	75°33'54,4"	**1207000**	16	8.36	99	9	4.8	0.402	18.5	0.245	0.756
Z-94	63°48'16,8"	75°33'47,2"	**19.6**	18	8.36	104	24	3.9	0.304	20.2	0.041	0.272
Z-95	63°48'29,7"	75°33'55,0"	**4.9**	17.8	7.4	98	31	4.1	0.305	26.0	0.045	0.732
Z-96*	63°48'30,2"	75°33'54,7"	**580586**	9.3	7.9	88	8	4.7	0.550	8.6	0.166	1.011

Table 1, continued.

	N	E	S, m²	T, °C	O_2, mg/L	O_2, % sat	R, µS cm^{-1}	pH	DIC, ppm	DOC, ppm	Cl, ppm	SO4, ppm
Z-97	63°47'39,0"	75°33'02,3"	**3**	19.6	7.9	91	18	4.34	0.285	21.9	0.032	0.316
Z-98	63°46'17,2"	75°40'58,6"	**0.79**	15.6	7.27	92	19	4.5	0.282	20.7	0.108	0.317
Z-99	63°46'18,5"	75°40'42,9"	**314**	17.9	6.44	86	N.D.	4.45	0.298	20.3	0.136	0.027
Z-100	63°46'14,4"	75°40'34,2"	**3.1**	15.7	6.7	84	N.D.	4.15	0.311	23.7	0.081	0.322
Z-101	63°46'14,4"	75°40'32,5"	**7850**	13.3	6.8	80	N.D.	4.0	0.347	10.0	0.055	0.252
Z-102	63°46'10,1"	75°40'21,5"	**4.9**	12.5	5.7	70	N.D.	3.6	0.353	28.8	0.151	0.465
Z-103	63°46'09,2"	75°40'11,4"	**961.6**	19.5	6.8	88	N.D.	4.2	0.291	20.9	0.075	0.318
Z-104	63°46'07,8"	75°40'07,0"	**0.13**	17.9	5.3	71	N.D.	3.6	0.304	45.0	0.182	0.619
Z-105	63°46'07,7"	75°40'04,4"	**706.5**	14.6	6.7	80	N.D.	4.2	0.294	18.4	0.037	0.218
Z-106	63°46'01,4"	75°39'57,0"	**12.6**	18.2	6.8	90	N.D.	4.1	0.270	22.4	0.043	0.305
Z-107	63°46'03,7"	75°39'54,3"	**196250**	15.6	6.8	85	N.D.	4.31	0.293	25.0	N.D.	N.D.

Table 1, continued.

	N	E	S, m²	T, °C	O$_2$, mg/L	O$_2$, % sat	R, μS cm^{-1}	pH	DIC, ppm	DOC, ppm	Cl, ppm	SO4, ppm
August												
Z-1(E)**	63°47'57,9"	75°33'49,2"	**1207000**	N.D.	N.D.	N.D.	N.D.	5.45	0.422	16.55	0.089	0.3259
Z-2*	63°48'11,1"	75°33'23,2"	**580586**	N.D.	N.D.	N.D.	N.D.	5.63	0.440	14.40	0.187	0.6155
Z-3(A)**	63°48'27,6"	75°32'29,3"	**503300**	N.D.	N.D.	N.D.	N.D.	4.88	0.376	13.86	0.111	0.2534
Z-4	63°51'32,11"	75°37'10,6"	**33000**	N.D.	N.D.	N.D.	N.D.	4.88	0.363	7.73	0.039	0.0804
Z-5	63°49'32,1"	75°34'00,6"	**74000**	N.D.	N.D.	N.D.	N.D.	4.92	0.429	12.8	0.423	0.1880
Z-6(B)**	63°47'15,2"	75°37'58,3"	**1396000**	N.D.	N.D.	N.D.	N.D.	6.20	2.470	11.7	0.480	0.1711
Z-7(C)**	63°47'06,7"	75°38'12,2"	**53630**	N.D.	N.D.	N.D.	N.D.	4.67	0.385	13.7	0.076	0.1023
Z-8	63°47'02,3"	75°38'02,5"	**6000**	N.D.	N.D.	N.D.	N.D.	4.41	0.370	27.7	0.156	0.342
Z-9	63°47'01,1"	75°39'05,5"	**359.8**	N.D.	N.D.	N.D.	N.D.	4.20	0.403	27.4	0.098	0.200
Z-10	63°46'56,8"	75°39'10,9"	**1481.9**	N.D.	N.D.	N.D.	N.D.	4.21	0.334	51.8	0.197	0.326
Z-11	63°46'53,8"	75°39'18,6"	**1766000**	N.D.	N.D.	N.D.	N.D.	5.28	0.392	8.4	0.182	0.283
Z-12	63°47'36,2"	75°33'10,0"	**1256**	N.D.	N.D.	N.D.	N.D.	4.66	0.392	11.6	0.048	0.104
Z-13	63°47'38,5"	75°33'07,1"	**1963**	N.D.	N.D.	N.D.	N.D.	4.16	0.570	35.4	0.090	0.306
Z-14	63°47'43,8"	75°33'12,5"	**1963**	N.D.	N.D.	N.D.	N.D.	4.33	0.310	18.5	0.037	0.114
Z-15 (D)**	63°47'45,9"	75°33'11,2"	**3485**	N.D.	N.D.	N.D.	N.D.	4.19	0.301	19.5	0.038	0.072
Z-16	63°47'49,3"	75°33'10,6"	**201.0**	N.D.	N.D.	N.D.	N.D.	4.16	0.386	35.7	0.077	0.119
Z-17	63°47'56,3"	75°31'26,1"	**2374.6**	N.D.	N.D.	N.D.	N.D.	4.94	0.341	52.9	1.178	0.486
Z-18	63°47'56,6"	75°31'21,9"	**707**	N.D.	N.D.	N.D.	N.D.	4.35	0.373	17.6	0.082	0.049
Z-19	63°47'56,0"	75°31'12,7"	**415**	N.D.	N.D.	N.D.	N.D.	4.17	0.335	23.4	0.088	0.091
Z-20	63°48'00,9"	75°30'54,8"	**78.5**	N.D.	N.D.	N.D.	N.D.	4.65	0.306	38.6	0.242	0.159
Z-21	63°47'58,9"	75°30'50,8"	**491**	N.D.	N.D.	N.D.	N.D.	4.50	0.319	35.6	0.118	0.245
Z-22	63°47'58,2"	75°30'53,8"	**7850**	N.D.	N.D.	N.D.	N.D.	4.25	0.316	31.0	0.157	3.115
Z-23	63°47'56,8"	75°30'43,7"	**4416**	N.D.	N.D.	N.D.	N.D.	4.56	0.300	28.7	0.084	3.116
Z-24	63°47'57,4"	75°30'33,9"	**6359**	N.D.	N.D.	N.D.	N.D.	4.35	0.321	18.9	0.142	0.126
Z-25	63°47'59,3"	75°30'35,1"	**5408**	N.D.	N.D.	N.D.	N.D.	4.88	0.312	18.6	0.073	0.164
Z-26	63°47'57,5"	75°30'30,8"	**314**	N.D.	N.D.	N.D.	N.D.	4.48	0.340	54.7	0.193	0.280

Table 1, continued.

	N	E	S, m²	T, °C	O_2, mg/L	O_2, % sat	R, μS cm^{-1}	pH	DIC, ppm	DOC, ppm	Cl, ppm	SO_4, ppm
Z-27	63°43'59,9"	75°49'48,3"	**2375**	N.D.	N.D.	N.D.	N.D.	5.88	0.865	9.3	0.031	2.016
Z-28	63°44'12,7"	75°48'55,6"	**3524**	N.D.	N.D.	N.D.	N.D.	6.10	1.251	15.3	0.197	0.183
Z-29	63°47'26,1"	75°33'50,5"	**1520**	N.D.	N.D.	N.D.	N.D.	5.54	0.465	22.8	0.766	0.246
Z-30	63°47'28,2"	75°33'51,8"	**31400**	N.D.	N.D.	N.D.	N.D.	5.59	0.360	38.2	0.608	4.797
Z-31	63°47'42,9"	75°31'32,4"	**5024**	N.D.	N.D.	N.D.	N.D.	5.66	0.357	10.6	0.055	0.855
October												
OZ-1	63°13'31,6"	75°43'32,6"	**96163**	N.D.	N.D.	N.D.	N.D.	4.21	1.552	48.2	0.181	0.110
OZ-2	63°13'22,6"	75°43'22,1"	**17663**	N.D.	N.D.	N.D.	N.D.	4.57	0.713	32.1	0.183	0.379
OZ-3	63°13'18,8"	75°43'22,1"	**491**	N.D.	N.D.	N.D.	N.D.	5.29	1.835	52.7	0.282	0.232
OZ-4	63°13'15,1"	75°43'19,0"	**70650**	N.D.	N.D.	N.D.	N.D.	4.69	0.618	12.3	0.128	0.153
OZ-5	63°13'16,4"	75°43'34,6"	**1963**	N.D.	N.D.	N.D.	N.D.	3.75	0.536	27.5	0.115	0.128
OZ-6	63°13'20,8"	75°43'44,8"	**12266**	N.D.	N.D.	N.D.	N.D.	4.29	0.445	14.1	0.078	0.133
OZ-7	63°13'16,5"	75°43'17,1"	**49063**	N.D.	N.D.	N.D.	N.D.	4.99	0.533	13.5	0.129	0.164
OZ-8	63°13'06,5"	75°43'22,4"	**707**	N.D.	N.D.	N.D.	N.D.	4.74	1.828	39.1	0.309	0.308
OZ-9	63°13'03,4"	75°43'15,7"	**2826**	N.D.	N.D.	N.D.	N.D.	4.33	0.488	17.0	0.106	0.037
OZ-10	63°13'23,2"	75°43'02,6"	**177**	N.D.	N.D.	N.D.	N.D.	4.52	3.492	35.4	1.252	0.178
OZ-11	63°47'54,1"	75°31'33,3"	**110**	N.D.	N.D.	N.D.	N.D.	3.99	0.723	24.3	0.541	0.036
OZ-12	63°48'03,0"	75°31'33,8"	**196250**	N.D.	9.3	86	N.D.	4.57	1.264	29.2	0.201	0.746

Table 1, continued.

	N	E	S, m^2	T, °C	O_2, mg/L	O_2, % sat	R, µS cm^{-1}	pH	DIC, ppm	DOC, ppm	Cl, ppm	SO_4, ppm
OZ-13	63°48'18,2"	75°31'30,4"	**196250**	N.D.	10.5/8.3	95/74	8	4.77	0.574	24.3	0.165	0.601
OZ-14	63°48'28,0"	75°31'28,7"	**707**	N.D.	12.3/10	100/94	6	4.21	0.460	16.8	0.122	0.060
OZ-15	63°48'36,8"	75°31'38,1"	**41527**	N.D.	8.8/7.2	74/64	N.D.	4.84	0.650	26.3	0.224	0.248
OZ-16(A)**	63°48'37,3"	75°32'28,2"	**503300**	N.D.	7.4/6.2	67/56	N.D.	4.87	0.581	13.7	0.194	0.314
OZ-17*	63°48'21,0"	75°33'08,6"	**580586**	N.D.	9.1/6.9	80/66	N.D.	5.01	0.507	15.3	0.284	0.316
OZ-18(E)**	63°48'15,2"	75°34'12,0"	**1207000**	N.D.	8.1/7.3	80/68	N.D.	4.69	0.495	13.7	0.193	0.708
OZ-19	63°47'52,9"	75°33'19,8"	**9499**	N.D.	8.6/5.8	78/55.2	N.D.	4.10	0.602	29.6	0.074	0.247
OZ-20(D)**	63°47'47,0"	75°33'11,3"	**3485**	N.D.	11.7/10.3	101/97	N.D.	4.01	0.596	24.9	0.179	0.052
OZ-21	63°47'47,2"	75°32'58,9"	**11304**	N.D.	10.1/4.7	92/44	N.D.	4.91	0.530	45.6	0.464	1.410
OZ-22	63°46'56,1"	75°38'53,7"	**2462**	N.D.	8.25/5.87	72/53	N.D.	3.96	0.508	28.6	0.246	1.566
OZ-23	63°46'58,4"	75°38'45,2"	**5024**	N.D.	4.2/3.34	38/30	N.D.	3.81	0.662	27.7	0.828	0.878
OZ-24	63°46'59,0"	75°38'33,8"	**3215**	N.D.	5.1/4.5	46/40	N.D.	3.99	0.595	16.5	0.140	0.121
OZ-25 (C)**	63°47'02,6"	75°38'21,2"	**53630**	N.D.	9.2/4.4	85/41	N.D.	4.06	0.556	16.3	0.095	0.204
OZ-26	63°47'10,8"	75°38'24,2"	**5672**	N.D.	8.3/4.0	75/38	N.D.	4.85	0.820	31.1	0.234	2.909
OZ-27	63°47'12,1"	75°38'34,64"	**17663**	N.D.	7.8/5.4	79/49	N.D.	3.87	0.466	33.1	0.164	0.535
OZ-28 (B)**	63°47'21,9"	75°38'28,2"	**1396000**	N.D.	9.75	87	N.D.	6.90	2.920	12.3	0.543	1.686
OZ-29	67°47'10,2"	75°38'51,1"	**28339**	N.D.	4.2/5.4	37/49	N.D.	3.98	0.488	37.5	0.170	0.606
OZ-30	63°47'04,2"	75°38'56,1"	**13267**	N.D.	4.2/5.8	37/51	N.D.	3.98	0.444	34.4	0.187	0.669
OZ-31	63°46'57,8"	75°39'02,1"	**962**	N.D.	4.5/3.9	40/35	N.D.	3.77	0.469	23.1	0.229	0.186
February												
LF1* bottom	63˚48'19.6"	75˚33'19.2"	**580586**	N.D.	N.D.	N.D.	N.D.	N.D.	0.496	30.3	0.792	3.440
LF4 bottom	63˚48'44.7"	75˚34'37.3"	**351335**	N.D.	N.D.	N.D.	19	4.655	0.778	19.0	0.235	1.678
LF5 bottom	63˚49'09.4"	75˚34'44.1"	**1743000**	N.D.	N.D.	N.D.	31	4.778	1.022	32.9	0.281	2.973

Footnote: Oxygen concentration in samples OZ-13 to OZ-31 represents surface/bottom values. Highlighted lakes (A, B, C, D, and E), **, were sampled during all open water seasons. *R* stands for specific conductivity and N.D. for non determined. * stands for a lake sampled during all four seasons.

Table 2. Distribution coefficient of soluble components between the lake water and the ice (average of 3 samples with 2 s.d.). The lower part of the ice column, formed in quasi-equilibrium with the remaining bottom water, was used for this estimation.

Element	**K_d (water)/(ice)**
DIC	**1.64±0.37**
DOC	**10.3±7.0**
Cl-	**7.58±3.0**
SO4	**44.1±10.9**
Na	**21.2±3.4**
Mg	**17.9±5.4**
Al	**93.1±32.9**
Si	**12.4±5.2**
K	**45.8±24.1**
Ca	**10.2±5.2**
Ti	**50±20**
V	**22.9±3.5**
Cr	**20.7±8.9**
Mn	**117±35**
Fe	**67.8±12.4**
Ni	**16.6±2.7**
Cu	**46.8±21.5**
Ga	**34.9±12.1**
As	**46.4±9.8**
Rb	**41.7±14.4**
Sr	**20.2±12.7**
Cd	**7.4±1.7**
Sb	**10.9±1.9**
Cs	**5.7±2.1**
Ba	**27.2±9.3**
La	**41.3±16.2**
Ce	**58.8±21.0**
Pr	**45.8±38.5**
Nd	**52.4±9.6**
Sm	**26.7±13.9**
Eu	**49.0±32.5**
Gd	**21.6±1.6**
Dy	**47.5±34.5**
Ho	**14.4±11.2**
Er	**23.4±7.9**
Yb	**19.1±12.4**
Pb	**41.5±12.2**
U	**11.5±2.9**

Table 3. Average concentrations and standard deviation (±2σ)of major and trace elements during different seasons of the year for two size classes of thermokarst lakes, 100-500000 m^2 and >500000 m^2. Considering all elements simultaneously, the difference between two size classes is statistically significant (p = 0.007, 0.0008 and 0.00007 for spring, summer and autumn) as follows from Wilcoxon t-test.

Element	**units**	**100–500000 m^2**			**>500000 m^2**			
		spring	**summer**	**autumn**	**spring**	**summer**	**autumn**	**winter**
DOC	mg/L	15.2±5.1	25.6±13.3	28±10.9	13.2±6.6	12.9±2.8	16.8±6.2	27.4±6.03
DIC	mg/L	0.38±0.07	0.42±0.2	0.79±0.67	0.5±0.18	0.49±0.17	1.15±0.93	0.77±0.21
Cl^-	mg/L	0.09±0.06	0.13±0.11	0.21±0.16	0.18±0.05	0.21±0.14	0.28±0.13	0.44±0.25
SO_4^{2-}	mg/L	0.37±0.2	0.44±0.41	0.43±0.38	0.69±0.27	0.33±0.15	0.75±0.5	2.33±0.65
Specific cond.	$\mu S\ cm^{-1}$	17.9±5.98	n.d.	7±1	9.8±1.47	n.d.	n.d.	25±6
pH		4.2±0.34	4.72±0.58	4.17±0.38	4.44±0.29	5.49±0.44	5.21±0.86	4.72±0.06
Be	µg/L	0.004±0.001	0.007±0.004	0.013±0.008	0.002±0.001	0.012±0.003	0.013±0.005	n.d.
B	µg/L	42.4±41.8	28.7±26.5	76.6±66.3	8.22±7.61	30.1±20.3	223±169	776±413
Na	µg/L	866±854	1220±1197	910±608	997±782	896±351	1396±925	6519±3818
Mg	µg/L	99.5±35	229±186	150±76.6	62.2±38.4	125±12.7	199±48.3	316±137
Al	µg/L	34.7±18.3	101±69.4	181±114	41.7±15.4	137±77.7	238±110	484±169
K	µg/L	124±123	207±203	302±227	256±144	272±95.6	447±253	2251±1254
Ca	µg/L	211.4±92.7	289±160	309±152	213±167	470±367	661±438	893±406
Ti	µg/L	0.512±0.27	1.16±0.664	1.76±1.3	0.569±0.229	4.46±2.75	4.44±4.01	3.63±1.24
V	µg/L	0.272±0.088	0.363±0.252	0.484±0.361	0.415±0.205	0.848±0.374	0.882±0.402	1.33±0.298
Cr	µg/L	0.138±0.075	0.366±0.166	0.477±0.274	0.157±0.045	0.457±0.125	0.651±0.238	1.14±0.423
Mn	µg/L	6.25±4.39	15.7±9.92	14.6±8.95	4.14±3.52	17.9±4.02	21.1±8.77	26.3±11.7
Fe	µg/L	84.4±57.3	251±162	230±111	127±63	273±240	336±146	447±108
Co	µg/L	0.037±0.018	0.103±0.05	0.141±0.064	0.029±0.016	0.095±0.035	0.093±0.039	0.215±0.034
Ni	µg/L	0.108±0.067	0.316±0.149	0.299±0.171	0.106±0.04	0.557±0.425	0.351±0.141	0.477±0.145
Cu	µg/L	0.252±0.207	0.47±0.289	0.789±0.691	0.208±0.07	0.634±0.439	1.2±0.768	3.56±2.01
Zn	µg/L	27.1±23.3	62.2±47	114±97.8	27.8±26.2	108±97.3	314±276	794±423
Ga	µg/L	0.01±0.004	0.023±0.016	0.042±0.033	0.007±0.004	0.037±0.023	0.06±0.031	0.146±0.069
As	µg/L	0.371±0.093	0.636±0.191	0.612±0.288	0.371±0.069	0.626±0.057	0.658±0.182	0.944±0.3
Rb	µg/L	0.147±0.141	0.213±0.205	0.328±0.294	0.275±0.069	0.388±0.166	0.92±0.536	2.07±0.963
Sr	µg/L	2.84±1.42	5.91±3.96	8±5.53	3.12±1.6	8.94±4.72	13±6.22	29.5±12.6
Zr	µg/L	0.243±0.2	0.1±0.068	0.216±0.165	0.488±0.011	0.309±0.138	0.612±0.359	2.06±1.8

Nb	µg/L	0.015±0.011	0.014±0.012	0.024±0.023	0.013±0.002	0.024±0.012	0.02±0.015	0.024
Mo	µg/L	0.012±0.007	0.01±0.009	0.021±0.015	0.023±0.008	0.021±0.003	0.021±0.009	0.033±0.017
Cd	µg/L	0.01±0.007	0.024±0.015	0.028±0.013	0.0005	0.017±0.01	0.025±0.019	0.04±0.008
Sb	µg/L	0.04±0.014	0.046±0.012	0.077±0.031	0.037±0.01	0.064±0.015	0.08±0.027	0.14±0.044
Cs	µg/L	0.008±0.007	0.008±0.007	0.007±0.006	0.003±0.002	0.013±0.007	0.023±0.013	0.027±0.011
Ba	µg/L	49.5±48.9	126.4±81.2	410±393	63.5±61.8	139±77.3	466±367	1107±446
La	µg/L	0.01±0.007	0.037±0.031	0.052±0.041	0.003±0.002	0.072±0.02	0.071±0.016	0.221±0.016
Ce	µg/L	0.021±0.014	0.09±0.083	0.122±0.114	0.001±0.0009	0.15±0.052	0.14±0.02	0.561±0.04
Pr	µg/L	0.004±0.003	0.011±0.01	0.016±0.015	n.d.	0.018±0.006	0.017±0.003	0.065±0.007
Nd	µg/L	0.016±0.011	0.047±0.045	0.059±0.055	0.028±0.007	0.078±0.026	0.074±0.011	0.215±0.022
Sm	µg/L	0.007±0.005	0.012±0.011	0.018±0.017	0.011±0.005	0.019±0.007	0.018±0.006	0.063±0.005
Eu	µg/L	0.013±0.012	0.019±0.018	0.036±0.034	0.022±0.018	0.014±0.005	0.035±0.032	0.142±0.052
Gd	µg/L	0.009±0.006	0.013±0.011	0.019±0.017	0.015±0.003	0.019±0.007	0.021±0.005	0.068±0.008
Dy	µg/L	0.011±0.009	0.012±0.009	0.016±0.015	0.023±0.004	0.019±0.005	0.02±0.005	0.061±0.012
Ho	µg/L	0.002±0.001	0.003±0.002	0.005±0.004	n.d.	0.004±0.002	0.004±0.0008	0.018±0.004
Er	µg/L	0.015±0.013	0.006±0.005	0.01±0.009	0.029±0.002	0.012±0.003	0.013±0.002	0.041±0.008
Tm	µg/L	0.002±0.001	0.002±0.001	0.002±0.001	n.d.	0.002±0.001	0.002±0.0009	0.009±0.001
Yb	µg/L	0.011±0.009	0.006±0.005	0.007±0.005	0.021±0.003	0.01±0.003	0.013±0.004	0.04±0.007
Lu	µg/L	0.002±0.001	0.002±0.001	0.002±0.001	n.d.	0.002±0.001	0.002±0.0006	0.01±0.005
Hf	µg/L	0.0065±0.0015	0.007±0.006	0.01±0.008	0.0034±0.0015	0.012±0.003	0.012±0.007	0.034±0.026
W	µg/L	0.016±0.009	0.083±0.081	0.115±0.112	0.018±0.004	0.059±0.046	0.068±0.054	0.026±0.019
Pb	µg/L	0.199±0.165	0.266±0.181	0.487±0.394	0.094±0.057	0.184±0.067	0.256±0.094	0.985±0.124
Th	µg/L	0.015±0.048	0.011±0.009	0.015±0.01	0.011±0.007	0.023±0.007	0.018±0.009	0.026±0.006
U	µg/L	0.003±0.002	0.006±0.005	0.009±0.008	n.d.	0.01±0.005	0.008±0.004	0.029±0.01